Z. Phys. C - Particles and Fields Manuscript-Nr.
(will be inserted by hand later)

Hadronic contributions to $g-2$ of the leptons and to the effective fine structure constant $\alpha(M_Z^2)$

S. Eidelman and F. Jegerlehner

[1] Budker Institute for Nuclear Physics, 630090 Novosibirsk, Russia
[2] Paul Scherrer Institute, CH-5232 Villigen PSI, Switzerland

Received: August 9, 1995/ Accepted: August 9, 1995

Abstract. The new experiment planned at Brookhaven to measure the anomalous magnetic moment of the muon $a_\mu \equiv (g_\mu - 2)/2$ will improve the present accuracy of 7 ppm by about a factor of 20. This requires a careful reconsideration of the theoretical uncertainties of the $g-2$ predictions, which are dominated by the error of the contribution from the light quarks to the photon vacuum polarization. This issue is crucial also for the precise determination of the running fine structure constant at the Z–peak as LEP/SLC experiments continue to increase their precision. In this paper we present an updated analysis of the hadronic vacuum polarization using all presently available e^+e^- data. This seems to be justified because previous work on the subject was based to some extent on preliminary or incomplete experimental data. Contributions from different energy ranges are presented separately for $g-2$ of the muon and the τ–lepton and for $\alpha(M_Z^2)$. We obtain the results $a_\mu^{\mathrm{had}\,*} = (725 \pm 16) \times 10^{-10}$ and $a_\tau^{\mathrm{had}\,*} = (351 \pm 10) \times 10^{-8}$, where the asterisk indicates the dressed (renormalization group improved) value. For the effective fine structure constant at $M_Z = 91.1888$ GeV we obtain $\Delta\alpha^{(5)}_{\mathrm{had}} = 0.0280 \pm 0.0007$ and $\alpha(M_Z^2)^{-1} = 128.896 \pm 0.090$. Further improvement in the accuracy of theoretical predictions which depend on the hadronic vacuum polarization requires more precise measurements of e^+e^- cross–sections at energies below about 12 GeV in future experiments.

1. Introduction

The anomalous magnetic moment of the muon has been measured with very high precision at the CERN Muon Storage Ring [1]. It is one of the best measured quantities in physics. As it can be calculated with high accuracy [2, 3, 4] it provides an extremely clean test of electroweak theory and may give us important hints on possible deviations from the Standard Model (SM)[5, 6, 7, 8]. The special interest comes about because a_ℓ ($\ell = e, \mu, \tau$) corresponds to a helicity flip coupling $\bar{\ell}_L \sigma_{\mu\nu} F^{\mu\nu} \ell_R$ which must vanish at the tree level for any fermion in any renormalizable field theory. In the SM it is thus a finite calculable quantity nonvanishing only due to quantum fluctuations. Another interesting feature is that a_ℓ is finite only if the $WW\gamma$–coupling is of the Yang-Mills type. In the limit $m_\ell \to 0$ regular contributions to a_ℓ vanish in the SM because ℓ_L does not couple to ℓ_R in this limit. This brings one power of m_ℓ into the effective $\bar{\ell}\ell\gamma$ vertex; a second power is due to the normalization to the lepton Bohr magneton $e/2m_\ell$.

The m_ℓ^2–dependence of the weak interaction and the vacuum polarization effects makes them completely unobservable for the electron. The effects are enhanced however by the large factor m_μ^2/m_e^2 for the muon relative to the electron. This enhancement is very welcome and happens for all kinds of new physics that could couple to photons and leptons. Therefore a_μ is an important tool for obtaining stringent upper bounds on new physics contributions. For the τ (see e.g. [9, 10]) there is an additional enhancement factor m_τ^2/m_μ^2 which magnifies the interesting effects. However, because of the short τ–lifetime, a measurement of a_τ is very difficult. Therefore one is still off by a few orders of magnitude in establishing its value experimentally. The best possibility to determine a_τ is by the leptonic radiative τ–decay $\tau^- \to e^- \bar{\nu}_e \nu_\tau \gamma$ which also provides the best present upper bound [11].

The present accuracy [1]

$$a_\mu^{\mathrm{exp}} = (11659230 \pm 85) \times 10^{-10}$$

allows us to test QED with very high precision. The theoretical prediction includes a number of terms of different origin. We may write

$$a_\mu^{\mathrm{the}} = a_\mu^{\mathrm{QED}} + a_\mu^{\mathrm{had}} + a_\mu^{\mathrm{weak}} + a_\mu^{\mathrm{new}} \ ,$$

where the first, and by far largest term, is from pure QED, a_μ^{had} denotes the virtual hadronic (quark) contribution, which will be studied in this paper, a_μ^{weak} summarizes the SM effects due to virtual W, Z and Higgs particle exchanges and a_μ^{new} stands for possible contributions from extensions of the SM. If we assume the last term to be zero we have the theoretical prediction [2]

Table 1. Comparison of estimates of $a_\mu^{\rm had} \times 10^{10}$ by different authors

$a_\mu^{\rm had} \times 10^{10}$	Author	Year [Ref.]
663 ± 85	Barger et al.	1975 [16]
702 ± 80	Calmet et al., Narison	1978 [17]
684 ± 11	Barkov et al.	1985 [18]
$707 \pm 6 \pm 16$	Kinoshita et al.	1985 [19]
$710 \pm 10 \pm 5$	Casas et al.	1985 [20]
$705 \pm 6 \pm 5$	Martinovič, Dubnička	1990 [21]
$724 \pm 7 \pm 26$	Jegerlehner	1991 [22]
$699 \pm 4 \pm 2$	Dubničková et al.	1992 [23]
$702 \pm 6 \pm 14$	This work	
$725 \pm 6 \pm 15$	RG improved	

$$a_\mu^{\rm the} = (11659192 \pm 18) \times 10^{-10} \ ,$$

and therefore at present we have

$$a_\mu^{\rm exp} - a_\mu^{\rm the} = (38 \pm 87) \times 10^{-10} \ .$$

With the precision attempted by the forthcoming Brookhaven experiment [12] one should be able to establish the weak SM contribution $a_\mu^{\rm weak} \simeq 20 \times 10^{-10}$, for example. In fact, however, such contributions may be concealed by the theoretical uncertainty which is of a similar size. The latter is dominated by the uncertainty of the hadronic contribution and therefore a careful analysis of the problem is of primary importance. The problem is that the low energy hadronic effects cannot be calculated in perturbative QCD and one has to rely on the semi-phenomenological dispersion theoretical approach [13, 14, 15] which allows us to compute $a_\mu^{\rm had}$ as an integral over experimental data from e^+e^- annihilation. The experimental errors of the data of course imply then a theoretical uncertainty of $g-2$ predictions.

A comparison of different results based at least partially on this approach is given in Tab. 1 which illustrates the present status.

The second quantity considered in this paper is the hadronic contribution $\Delta\alpha_{\rm had}^{(5)}(M_Z^2)$ of the 5 light quark flavors to the shift of the fine structure constant from the Thomson limit to the Z–resonance $\Delta\alpha = 1 - \alpha/\alpha(M_Z^2)$. This quantity can also only be estimated reliably in terms of the experimental e^+e^- data with corresponding uncertainties. The effective fine structure constant $\alpha(s)$ plays a crucial role in precision physics at all energy scales beyond the very low energy region. It is particularly important for all physics of the weak gauge bosons, as being studied currently at LEP and SLC. Almost all SM predictions of observables in terms of α, G_μ and M_Z, the most precise set of input parameters available, depend on $\Delta\alpha(s)$. Again, the uncertainty of $\Delta\alpha_{\rm had}^{(5)}(M_Z^2)$ is a limiting factor which obscures the interpretation of precision measurements at a certain level. In fact, for the leptonic effective weak mixing parameter $\sin^2\theta_{\rm eff}^{\rm lept}(M_Z)$, which is determined in $e^+e^- \to \ell^+\ell^-$ at the Z-resonance, the LEP collaboration [24] has reached an experimental error $\delta\sin^2\theta_{\rm eff}^{\rm lept} \simeq 0.0004$ which is only slightly larger than the hadronic uncertainty of about 0.0003 of the SM prediction for this quantity. It thus has become a very crucial question whether it is possible to reduce the error of $\Delta\alpha_{\rm had}^{(5)}(M_Z^2)$ further and what the perspectives are in the future. The present situation is summarized by the results in Tab. 2.

Table 2. Comparison of estimates of $\Delta\alpha_{\rm had}^{(5)}(M_Z^2)$ by different authors

$\Delta\alpha_{\rm had}^{(5)}(M_Z^2)$	Author	Year [Ref.]
0.0285 ± 0.0007	Jegerlehner	1986 [25]
0.0283 ± 0.0012	Lynn et al.	1987 [26]
0.0287 ± 0.0009	Burkhardt et al.	1989 [27]
0.0282 ± 0.0009	Jegerlehner	1991 [28]
0.02666 ± 0.00075	Swartz	1994 [29]
0.02732 ± 0.00042	Martin and Zeppenfeld	1994 [30]
0.0280 ± 0.0007	This work	

Note that some of the values have been shifted by

$$\frac{\alpha}{3\pi}\frac{22}{3}\,(1+\frac{\alpha_s}{\pi})\;\ln(M_Z'/M_Z)$$

from the pre–LEP reference value $M_Z = 93$ GeV to the current value of M_Z. Ref. [26] quotes $\Delta\alpha_{\rm had}^{(5)}(-Q_0^2) = 0.0145 \pm 0.0012$ for $Q_0^2 = 79$ GeV^2. We have added $\Delta\alpha_{\rm had}^{(5)}(M_Z^2) - \Delta\alpha_{\rm had}^{(5)}(-Q_0^2) = 0.0138$ which is obtained by using 3rd order perturbative QCD. For a comparison of the earlier results [31] we refer to [25]. The differences are mainly due to a different treatment of the systematic errors and/or different model assumptions. The present situation justifies a reconsideration of the problem.

To calculate the necessary dispersion integrals below we prefer to use direct integration over the experimental values of cross sections. In this approach one can take into account uncertainties of separate measurements in a straightforward manner. The alternative method which was used in most of the previous works is to make a fit of the experimental points within some model and integrate the arising parametrization of the data. This procedure inevitably leads to a model dependence and it is not clear how experimental errors especially systematic uncertainties can be taken into account.

The two recent papers [29, 30] appeared while we were writing up this update. We have added some remarks which should clarify at least part of the discrepancies between these papers and the present analysis which yields results consistent with previous ones (e.g. [28]).

In Secs. 2 and 3 we will briefly review how the hadronic contributions to a_ℓ and $\Delta\alpha$ are determined by the e^+e^- data. Details on the evaluation of the dispersion integrals and the treatment of the errors are discussed in Sec. 4. In Sec. 5 we describe the e^+e^- data which we use in our analysis and in Sec. 6 we present the results. A brief summary and outlook follows in Sec. 7.

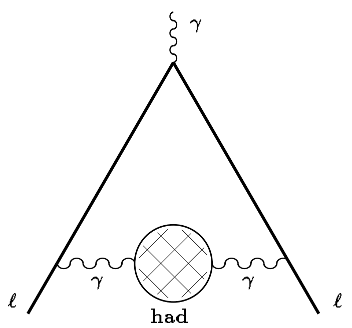

Fig. 1. Leading hadronic vacuum polarization contribution to $g-2$ of a lepton

2. Hadronic contributions to the anomalous magnetic moments of the leptons

The leading hadronic contribution to $g-2$ is due to the photon vacuum polarization insertion into the vertex diagram of the electromagnetic vertex of a lepton. The corresponding diagram is shown in Fig. 1.

The "blob" represents the irreducible photon self-energy. Subleading hadronic contributions are obtained by multiple self-energy insertions or insertions of irreducible light-by-light scattering (4γ) or higher amplitudes [19, 32]. We will not discuss such subleading terms in this paper unless stated otherwise.

As already mentioned before, the low energy hadron effects which are needed here, and in principle are determined by QCD, cannot be obtained by using perturbation theory. Fortunately, this contribution may be calculated in terms of the experimental total cross section $\sigma_{\rm had} = \sigma(e^+e^- \to \text{hadrons})$ of e^+e^- annihilation into any hadronic state by using the familiar dispersion integral [13, 14, 15]

$$\begin{aligned} a_\mu^{\rm had} &= \frac{1}{4\pi^3}\int_{4m_\pi^2}^{\infty} ds\, \sigma^{(0)}_{\rm had}(s)\, K(s) \\ &= \left(\frac{\alpha m_\mu}{3\pi}\right)^2 \int_{4m_\pi^2}^{\infty} ds\, \frac{R(s)\,\hat{K}(s)}{s^2} \end{aligned} \tag{1}$$

which can be evaluated by using the experimental data for $\sigma_{\rm had}(s)$ or $R(s)$ up to some sufficiently high energy, e.g., $E_{\rm cut} = 40$ GeV, and by perturbative QCD for the high energy tail.

For the moment we are interested in calculating the contribution from the irreducible photon self-energy, in which case we have to use the "undressed" ($\equiv$ lowest order with respect to QED) hadronic cross section

$$\sigma^{(0)}_{\rm had}(s) = \sigma_{\rm had}(s)\,(\alpha/\alpha(s))^2 \ . \tag{2}$$

We refer to the Appendix for a brief discussion of "dressed" versus "undressed" quantities in dispersion relations.

The second form in Eq. (1) is convenient for the evaluation of contributions at higher energies. It is an expression in terms of the cross-section ratio

$$R(s) = \frac{\sigma_{\rm tot}(e^+e^- \to \gamma^* \to \text{hadrons})}{\sigma(e^+e^- \to \gamma^* \to \mu^+\mu^-)} \ . \tag{3}$$

Note that $R(s)$, by the proper definition according to Eq. (3), is the *ratio of the total cross sections* which is determined by QCD. In perturbative QCD we have [33]

$$\begin{aligned} R(s) &= 3\sum_f Q_f^2 \sqrt{1-4m_f^2/s}\,(1+2m_f^2/s) \\ &\quad \times \left(1 + a + c_1 a^2 + c_2 a^3 + \cdots\right) \end{aligned} \tag{4}$$

where Q_f and m_f denote the charge and mass of the quark, respectively, $a = \alpha_s(s)/\pi$ with $\alpha_s(s)$ the strong coupling constant, and

$$\begin{aligned} c_1 &= 1.9857 - 0.1153 N_f \\ c_2 &= -6.6368 - 1.2002 N_f - 0.0052 N_f^2 \\ &\quad -1.2395\,(\textstyle\sum Q_f)^2/(3\sum Q_f^2) \end{aligned}$$

in the $\overline{MS}$ scheme. N_f is the number of active flavors. This result is applicable about 1 GeV above the resonances and at sufficiently high energies and will be used in particular to calculate the high energy tail of Eq. (1). We will assume a top mass of 173 GeV [24] for the calculation of the perturbative tail. As a check we also will compare the experimental data in the region above the ψ–resonances with the calculation of $R(s)$ presented recently in Ref. [34], which is improved by charm and bottom mass effects.

Usually experiments do not determine R as a ratio of the total cross sections as given by Eq. (3). Rather the hadronic experimental cross section is first corrected for QED effects [35, 36, 37, 38], which include bremsstrahlung as well as vacuum polarization corrections. The latter account for the running of the fine structure constant $\alpha(s)$. After these corrections have been applied $\sigma_{\rm tot}$ is divided by the Born cross section $\sigma_0(e^+e^- \to \gamma^* \to \mu^+\mu^-) = \frac{4\pi\alpha^2}{3s}$ so that

$$R(s) = \frac{\sigma_{\rm tot}(e^+e^- \to \gamma^* \to \text{hadrons})^{\rm cor}_{\rm exp}}{\sigma_0(e^+e^- \to \gamma^* \to \mu^+\mu^-)} \ .$$

Note that, the experimental cross section $\sigma(e^+e^- \to \gamma^* \to \mu^+\mu^-)$ never appears here and is used by careful groups to check how good normalization is (see e.g., [39]). The question of how R has been determined precisely in a given experiment is not always clear. We will comment on this point when discussing the data below.

A renormalization group (RG) improvement of the result may be obtained by resumming the multiple irreducible self-energy insertions, which is equivalent to using the full photon propagator in Fig. 1. As shown in the Appendix, this is simply achieved by using the physical cross section $\sigma_{\rm had}(s)$ or, equivalently, the "dressed" R–function $R(s)^{\rm dressed} = R(s)(\alpha(s)/\alpha)^2$ under the dispersion integral Eq. (1).

Turning back to Eq. (1), the kernel $K(s)$ may conveniently be written in terms of the variable

$$x = \frac{1-\beta_\mu}{1+\beta_\mu}\ ,\quad \beta_\mu = \sqrt{1-4m_\mu^2/s}$$

and is given by

$$K(s) = \frac{x^2}{2}\,(2-x^2)$$

$$+\frac{(1+x^2)(1+x)^2}{x^2}\left(\ln(1+x)-x+\frac{x^2}{2}\right)$$
$$+\frac{(1+x)}{(1-x)}\,x^2\ln(x)\ . \qquad (5)$$

Note that the function

$$\hat{K}(s)=\frac{3s}{m_\mu^2}K(s)$$

is bounded: it increases monotonically from 0.63 at threshold $s=4m_\pi^2$ to 1 at $s\to\infty$. It should be noted that for small x the calculation of the function $K(s)$, in the form given above, is numerically instable and we instead use the asymptotic expansion (used typically for $x\leq 0.0006$)

$$K(s)=\left(\frac{1}{3}+\left(\frac{17}{12}+\left(\frac{11}{30}+\left(-\frac{1}{10}+\frac{3}{70}x\right)x\right)x\right)x\right)x$$
$$+\frac{1+x}{1-x}\,x^2\ln(x)\ .$$

Other representations of $K(s)$, like the simpler–looking form

$$K(s)=\frac{1}{2}-r+\frac{1}{2}r\,(r-2)\,\ln(r)$$
$$+\left(1-2r+\frac{1}{2}r^2\right)\,\ln(x)/\beta_\mu\ \ ,$$

with $r=s/m_\mu^2$, are much less suitable for numerical evaluation because of much more severe numerical cancellation (even less stable is the representation utilized in [23]).

The representation Eq. (5) of $K(s)$ is valid for the muon (or electron) where we have $s>4m_\mu^2$ in the domain of integration $s>4m_\pi^2$, and x is real, and $0\leq x\leq 1$. For the τ Eq. (5) applies for $s>4m_\tau^2$. In the region $4m_\pi^2<s<4m_\tau^2$, where $0<r=s/m_\tau^2<4$, we may use the form

$$K(s)=\frac{1}{2}-r+\frac{1}{2}r\,(r-2)\,\ln(r)$$
$$-\left(1-2r+\frac{1}{2}r^2\right)\,\varphi/w \qquad (6)$$

with $w=\sqrt{4/r-1}$ and $\varphi=2\tan^{-1}(w)$.

3. Hadronic contributions to the running of the effective fine structure constant

The effective fine structure constant at scale $\sqrt{s}$ is given by

$$\alpha(s)=\frac{\alpha}{1-\Delta\alpha(s)}\ \ , \qquad (7)$$

where α is the fine structure constant and $\Delta\alpha$ is the photon vacuum polarization contribution. In terms of the one particle irreducible photon self-energy $\Pi_\gamma(s)=s\Pi'_\gamma(s)$ we have

$$\Delta\alpha(s)=\Pi'_\gamma(0)-\mathrm{Re}\ \Pi'_\gamma(s)\ \ , \qquad (8)$$

which for $s=M_Z^2$, for example, is large due to the large change in scale going from zero momentum (Thomson limit) to the Z-mass scale $\mu=M_Z$. In perturbation theory, the leading light fermion ($m_f\ll M_W,\sqrt{s}$) contribution is given by

$$\Delta\alpha(s)=\sum_f$$
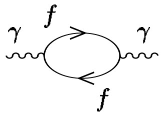

$$=\frac{\alpha}{3\pi}\sum_f Q_f^2 N_{cf}\ (\ln\frac{s}{m_f^2}-\frac{5}{3})\ \ , \qquad (9)$$

with Q_f the fermion charge and N_{cf} the color factor, 1 for leptons and 3 for quarks. We distinguish the contributions from the leptons, for which Eq. (9) is appropriate, the five light quarks and the top

$$\Delta\alpha=\Delta\alpha_l+\Delta\alpha^{(5)}_{\mathrm{had}}+\Delta\alpha_{\mathrm{top}}\ . \qquad (10)$$

Since the top quark is heavy we cannot use the light fermion approximation for it. A very heavy top in fact decouples like

$$\Delta\alpha_{\mathrm{top}}\simeq-\frac{\alpha}{3\pi}\frac{4}{15}\frac{M_Z^2}{m_t^2}\to 0$$

when $m_t\gg M_Z$.

A serious problem is the low energy contributions of the five light quarks u, d, s, c and b which cannot be reliably calculated by using perturbative QCD. Fortunately, again one can evaluate this hadronic term $\Delta\alpha^{(5)}_{\mathrm{had}}$ from hadronic e^+e^-–annihilation data by using a dispersion relation together with the optical theorem which results in the integral [40, 31]

$$\Delta\alpha^{(5)}_{\mathrm{had}}(M_Z^2)=-\frac{M_Z^2}{4\pi^2\alpha}\ \mathrm{Re}\int_{4m_\pi^2}^{\infty}ds\frac{\sigma^{(0)}_{\mathrm{had}}(s)}{s-M_Z^2-\mathrm{i}\varepsilon}$$
$$=-\frac{\alpha M_Z^2}{3\pi}\ \mathrm{Re}\int_{4m_\pi^2}^{\infty}ds\frac{R(s)}{s(s-M_Z^2-\mathrm{i}\varepsilon)}\ ,\qquad (11)$$

which is very similar to the one we encountered for $g-2$ in Eq. (1). The only difference is the different weight-function multiplying $R(s)$ under the integral. Since Eq. (1) has an extra factor $1/s$ at low s the low energy data play a dominant role for a_μ while Eq. (11) gets significant contributions from a broad energy range up to about $E\simeq M_Z/2$, as we shall see below.

Note that the remarks made earlier about the proper definition of $R(s)$ apply here as well.

Above the Υ energy we apply a correction factor for $\gamma-Z$ mixing to $R(s)^{\mathrm{exp}}$. The correction for the Z–exchange contribution is given by the ratio $c_{QQ}/c_{\gamma Z}$ where

$$c_{QQ}=\sum_f Q_f^2=\frac{11}{9}\ \ ,$$

$$c_{\gamma Z}=c_{QQ}-2v_e c_{Qv}P(s)+c_e c_f P(s)^2\ \ .$$

We denoted the Z–pole factor by

$$P(s)=\frac{\sqrt{2}G_\mu M_Z^2}{16\pi\alpha}\frac{s}{s-M_Z^2}$$

and the coefficients are determined by the $Zf\bar{f}$ couplings v_f and a_f as follows:

$$\begin{aligned} c_{Qv} &= \sum_f Q_f v_f &&= \tfrac{7}{3} - \tfrac{44}{9}\sin^2\Theta_W \\ c_e &= v_e^2 + a_e^2 &&= 2 - 8\sin^2\Theta_W + 16\sin^4\Theta_W \\ c_f &= \sum_f (v_f^2 + a_f^2) &&= 10 - \tfrac{56}{3}\sin^2\Theta_W + \tfrac{176}{9}\sin^4\Theta_W\ . \end{aligned}$$

In our normalization $v_e = -1 + 4\sin^2\Theta_W$. We use the LEP values $M_Z = 91.1888$ GeV and $\sin^2\Theta_W = \sin^2\theta_{\rm eff}^{\rm lept}(M_Z) = 0.2322$ [24] for numerical estimates.

4. Evaluation of the dispersion integral

In order to obtain a conservative estimate of the relevant integrals we try to rely on the experimental data as much as possible and integrate directly the data points by joining them by straight lines (trapezoidal rule). In the low energy region it is customary to present the $\pi^+\pi^-$ and $\rho \to \pi^+\pi^-$ data in terms of the absolute square of the pion form-factor $|F_\pi(s)|^2$ which is related to the cross section by

$$\sigma(e^+e^- \to \pi^+\pi^-) = \frac{\pi}{3}\frac{\alpha^2\beta_\pi^3}{s}|F_\pi(s)|^2$$

or

$$R_{\pi\pi} = \frac{\beta_\pi^3}{4}|F_\pi(s)|^2 \tag{12}$$

where $\beta_\pi = (1 - 4m_\pi^2/s)^{1/2}$ is the pion velocity. In contrast to previous works which were using Gounaris-Sakurai [41] kind of parametrizations we will rely on the direct integration of the data in order not to obscure the error estimates. The definition of the pion form factor is similar in spirit to the one for $R(s)$. In principle, it is defined as a ratio of hadronic to leptonic cross sections such that it corresponds to a purely hadronic matrix element. For most of the low energy experiments (in particular the Novosibirsk VEPP-2M ones) R was calculated as follows [38]: first the hadronic cross section was obtained. Radiative corrections were applied which included lepton vacuum polarization only. And then the corrected hadronic cross section was divided by the muon cross section calculated using the constant low energy α. The more precise accounting of using the running α with the inclusion of hadronic vacuum polarization leads to a numerically very small (a_μ) or negligible ($\Delta\alpha$) difference. For consistency we apply the factor $(1+2\Delta\alpha_l(s))(\alpha/\alpha(s))^2$ to the pion form factor to account for this missing correction. The remarks made here for $\pi^+\pi^-$ apply as well for the K^+K^- and K_SK_L form-factors.

4.1. Resonances

A few exceptions from the direct integration are the narrow resonances ω, ϕ, the J/ψ family (6 states) and the Υ family (6 states). Here we can safely use the parametrization as Breit-Wigner resonances

$$\sigma_{\rm BW}(s) = \frac{12\pi}{M_R^2}\frac{\Gamma_{ee}}{\Gamma_R}\frac{M_R^2\Gamma_R\Gamma(s)}{(s-M_R^2)^2 + M_R^2\Gamma^2(s)} \tag{13}$$

or as a zero width resonance

$$\sigma_{\rm NW}(s) = \frac{12\pi^2}{M_R}\Gamma_{ee}\,\delta(s-M_R^2) \tag{14}$$

using resonance parameters from the Review of Particle Properties [42]. The s–dependent width is defined by the imaginary part of the irreducible self–energy of the resonance propagator as ${\rm Im}\Pi(s) = M_R\Gamma(s)$. Sufficiently far above the thresholds it behaves like

$$\Gamma(s) \simeq s/M_R^2\,\Gamma_R \quad \text{where} \qquad \Gamma_R = \Gamma(M_R^2)\ . \tag{15}$$

The procedure of calculating widths for the narrow resonances of the J/ψ and Υ families is described in the Review of Particle Properties, e.g., in the 1994 edition, on page 1661. The particle data group (PDG) lists "dressed"(i.e. physical) widths $(\Gamma, \Gamma_{ee}, \cdots)$ rather than lowest order ones $(\Gamma^{(0)}, \Gamma_{ee}^{(0)}, \cdots)$. This convention exists since the 1988 edition of the Review of Particle Properties [43], and was triggered by the articles Refs. [44], [45] and [46] which pointed out that, in the past, different experiments have been using different conventions which depended on the different treatment of the radiative corrections. A discussion of the radiative corrections which were performed by different experiments for the Υ resonances may be found in Ref. [44] where consistent world averages for the dressed widths are calculated by appropriate rescaling of the peaks of the resonances. In Ref. [46] the J/ψ and the Υ resonances were refitted using state of the art calculations for resonance line-shapes as they have been developed for precision physics at the Z-resonance, using Eq. (13) with $\Gamma(s) = s/M_R^2\,\Gamma_R$. Note that the convention mentioned above is employed by the authors themselves. The PDG only lists the results of original papers and averages them.

In terms of the physical ("dressed") widths resonance contributions to the R–values are given by

$$R_{\rm BW} = \frac{9}{\alpha^2(s)}\frac{s}{M_R^2}\frac{\Gamma_{ee}}{\Gamma_R}\frac{M_R^2\Gamma_R\Gamma(s)}{(s-M_R^2)^2 + M_R^2\Gamma^2(s)} \tag{16}$$

and correspondingly for the narrow resonance approximation. The latter is used only for calculating the resonance contributions to a_ℓ. It should be noted that the Breit–Wigner formula itself, valid in the vicinity of the resonance, is a result of summing over all quark vacuum polarization diagrams with any number of loops.

For the ω and the ϕ we proceed as described in Ref. [47] (see also [48]) and use the relativistic Breit–Wigner form with a s–dependent width

$$\begin{aligned} \Gamma_\omega(s) &= \Gamma(\omega\to 3\pi, s) + \Gamma(\omega \to \pi^0\gamma, s) + \Gamma(\omega \to 2\pi, s) \\ &= \frac{s}{M_\omega^2}\Gamma_\omega \left\{ \quad Br(\omega \to 3\pi)\frac{F_{3\pi}(s)}{F_{3\pi}(M_\omega^2)} \right. \\ &\qquad + Br(\omega\to\pi^0\gamma)\frac{F_{\pi\gamma}(s)}{F_{\pi\gamma}(M_\omega^2)} \\ &\qquad \left. + Br(\omega \to 2\pi)\frac{F_{2\pi}(s)}{F_{2\pi}(M_\omega^2)} \right\} \end{aligned}$$

$$\begin{aligned} \Gamma_\phi(s) &= \Gamma(\phi \to K^+K^-, s) + \Gamma(\phi \to K_SK_L, s) \\ &\quad + \Gamma(\phi \to 3\pi, s) + \Gamma(\phi\to\pi^0\gamma, s) + \Gamma(\phi \to \eta\gamma, s) \end{aligned}$$

$$= \frac{s}{M_\phi^2}\Gamma_\phi \left\{ Br(\phi \to K^+K^-)\frac{F_{K^+K^-}(s)}{F_{K^+K^-}(M_\phi^2)} \right.$$
$$+Br(\phi \to K_S K_L)\frac{F_{K_S K_L}(s)}{F_{K_S K_L}(M_\phi^2)}$$
$$+Br(\phi \to 3\pi)\frac{F_{3\pi}(s)}{F_{3\pi}(M_\phi^2)}$$
$$+Br(\phi \to \pi^0\gamma)\frac{F_{\pi\gamma}(s)}{F_{\pi\gamma}(M_\phi^2)}$$
$$\left. +Br(\phi \to \eta\gamma)\frac{F_{\eta\gamma}(s)}{F_{\eta\gamma}(M_\phi^2)} \right\} \quad (17)$$

where $Br(V \to X)$ denotes the branching fraction for the channel X and $F_X(s)$ is the phase space function for the corresponding channel normalized such that $F_X(s) \to const$ for $s \to \infty$. For the two-body decays $V \to P_1P_2$ we have $F_{P_1P_2}(s) = (1-(m_1+m_2)^2/s)^{3/2}$. The channel $V \to 3\pi$ is dominated by $V \to \rho\pi \to 3\pi$ and this fact is used when calculating $F_{3\pi}(s)$ [48]. Before extracting the width, radiative corrections according to Bonneau and Martin [35] or Kuraev and Fadin [38] have been performed which include subtracting the electron contribution to the vacuum polarization. In these cases the correction to be applied is $(1+2\Delta\alpha_e(s))(\alpha/\alpha(s))^2$ and not the full one.

4.2. The $\pi^+\pi^-$ threshold region

Experimental data are poor below about 400 MeV because the cross section is suppressed near the threshold. Because of the $1/s^2$ weight factor for small s in Eq. (1) we have to worry whether there could not be a relevant contribution missing. Here results from chiral expansion of the pion form factor [49] can be used (see also Ref. [20]).

To a good approximation the relevant vector form factor is given by

$$F_V^{\mathrm{CHPT}} \simeq 1 + \frac{1}{6} < r^2 >_V^\pi \cdot s \; + \; c_V^\pi \cdot s^2 \quad (18)$$

with $< r^2 >_V^\pi = 0.427 \pm 0.010\,\mathrm{fm}^2$ and $c_V^\pi = 4.1^{+0.2}_{-0.6}\,\mathrm{GeV}^{-4}$. The pion charge radius used here was determined from the precise spacelike data in Ref. [50]. We have used the value obtained from fits with a free normalization. The error includes the 0.9% systematic error of the data. The crucial point here is that the threshold behavior is severely constrained by the chiral structure of QCD via the rather precise data for the pion form factor in the spacelike region. The convergence of the momentum expansion can be improved by using the Padé approximants rather than the asymptotic expansion itself which is denoted by [0,2] in Padé terminology. With the information we have on the expansion coefficients we may obtain the [2,0] form

$$F_V^{\mathrm{CHPT}} \simeq 1/(1 - c_1 \cdot s \; - \; (c_2 - c_1^2) \; \cdot s^2) \, , \quad (19)$$

with $c_1 = \frac{1}{6} < r^2 >_V^\pi$ and $c_2 = c_V^\pi$; or the [1,1] form

$$F_V^{\mathrm{CHPT}} \simeq (1 + \; (c_1 - c_2/c_1) \; \cdot s)/(1 - \; (c_2/c_1) \; \cdot s) \, , \quad (20)$$

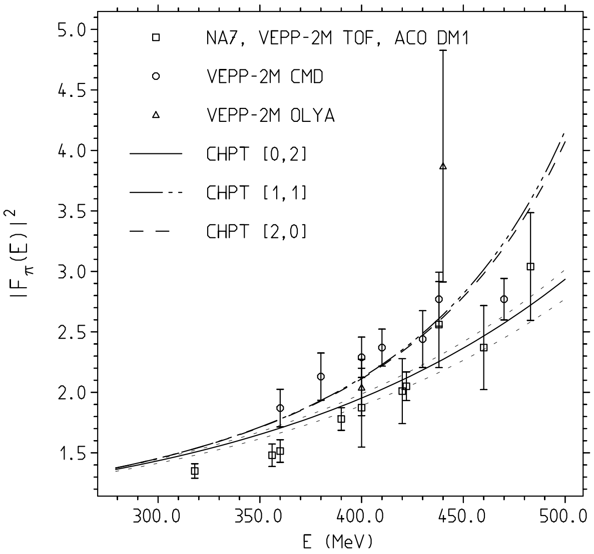

Fig. 2. The $e^+e^- \to \pi^+\pi^-$ data near threshold compared with the prediction of the pion form factor $|F_\pi(s)|^2$ for timelike $s = E^2$ from chiral expansion to two-loop order [49]. [1,1] and [2,0] denote Padé improvements

which agree with (18) when expanded in s up to terms of unknown higher orders. The difference obtained from the different representations is the "model" error, uncertainties due to missing higher order terms.

The results are shown in Fig. 2 and provide a good description of the data in the timelike region.

4.3. Estimate of the error

While statistical errors are added in quadrature throughout in our analysis the systematic errors of an experiment have to be added linearly. Usually the experiments give systematic errors as a relative systematic uncertainty and the systematic error to be added linearly is given by the central value times the relative uncertainty. For data from different experiments the combination of the systematic errors is more problematic. If one would add systematic errors linearly everywhere, the error would be obviously overestimated since one would not take into account the fact that independent experiments have been performed. Since we are interested in the integral over the data only, a natural procedure seems to be the following: for a given energy range (scan region) we integrate the data points for each individual experiment and then take a weighted mean, based on the quadratically combined statistical and systematic error, of the experiments which have been performed in this energy range. By doing so we have assumed that different experiments have independent systematic errors, which of course often is only partially true[1]. The problem with this method is

[1] If there are known common errors, like the normalization errors for experiments performed at the same facility, one has to add the common error after averaging. In some cases we correct for possible common errors by scaling up the systematic error appropriately.

that there exist regions where data are sparse yet the cross section varies rapidly, like in the ρ-resonance region. The applicability of the trapezoidal rule is then not reliable, but taking other models for the extrapolation introduces another source of systematic errors. It was noticed some time ago in Ref. [52] that fitting data to some function by minimizing χ^2 may lead to misleading results[2] and we insist on avoiding this kind of problems.

In order to start from a better defined integrand we do better to combine all available data points into a single dataset. If we would take just the collection of points as if they were from *one* experiment we not only would get a too pessimistic error estimate but a serious problem could be that scarcely distributed precise data points do not get the appropriate weight relative to densely spaced data point with larger errors. What seems to be more adequate is to take for each point of the combined set the weighted average of the given point and the linearly interpolated points of the other experiments:

$$\bar{R} = \frac{1}{w} \sum_i w_i R_i$$

with total error $\delta_{\rm tot} = 1/\sqrt{w}$, where $w = \sum_i w_i$ and $w_i = 1/\delta^2_{i\ \rm tot}$. By $\delta_{i\ \rm tot} = \sqrt{\delta^2_{i\ \rm sta} + \delta^2_{i\ \rm sys}}$ we denote the combined error of the individual measurements. In addition, to each point a statistical and a systematic error is assigned by taking weighted averages of the squared errors:

$$\delta_{\rm sta} = \left(\frac{1}{w} \sum_i w_i\, \delta^2_{i\ \rm sta}\right)^{1/2} , \quad \delta_{\rm sys} = \left(\frac{1}{w} \sum_i w_i\, \delta^2_{i\ \rm sys}\right)^{1/2} .$$

There is of course an ambiguity in separating the well–defined combined error into a statistical and a systematic one. We may also calculate separately the total error and the statistical one and obtain a systematic error $\delta_{\rm sys} = \sqrt{\delta^2_{\rm tot} - \delta^2_{\rm sta}}$. Both procedures give very similar results. We also calculate $\chi^2 = \sum_i w_i\ (R_i - \bar{R})^2$ and compare it with $N-1$, where N is the number of experiments. Whenever $S = \sqrt{\chi^2/(N-1)} > 1$, we scale the errors by the factor S, unless there are plausible arguments which allow one to discard inconsistent data points.

5. The e^+e^- data and the origin of systematic errors

Some general comments concerning the R determination are in order. In the ideal case one directly identifies each possible annihilation channel and measures its cross section. After that R is obtained as a sum of all separate contributions. We will call such an approach an "exclusive" one. One should be careful, however, while estimating the resulting systematic uncertainty since systematic uncertainties of separate channels may contain common parts like, e.g., normalization uncertainties. There may also be some model uncertainties arising from the fact that for each specific channel one has to assume some specific mechanism of the production of final particles, for example, for the production of four pions, $\omega\pi$, $a_1\pi$, $\rho\pi\pi$ etc., while in reality particles can be produced by different mechanisms. In a more realistic case identification of separate channels is not possible. One observes a certain number of multi-hadronic events of different types, for example, 2 charged particles, 2 charged particles plus n photons, 3 charged particles etc., assumes some mechanism of multi-hadron production and calculates within it a detection efficiency of observing any configuration of charged particles and photons. Minimizing χ^2 one obtains then the cross sections of separate channels and their sum gives a total cross section. In old experiments, pion production with an invariant phase space distribution was used as a mechanism of particle production (see, e.g. [79]). Lately the LUND model [53] has been used for detection efficiency determination. Here again additional model uncertainties arise. The value of R determined by such an "inclusive" method usually yields the total cross section not including production of two-body final states. One should also take into account that there may be production channels "invisible" to some experiments, like, for example, those having only neutral particles in the final state. Some of them may be accounted for by using isospin symmetry. For example, the cross section of the reaction $e^+e^- \to \pi^+\pi^-3\pi^0$ is equal to one half of that for $e^+e^- \to 2\pi^+2\pi^-\pi^0$, independently of the production mechanism. Such corrections although small will influence the central value of the calculated integral and will also contribute to the systematic uncertainty.

Since 1985 when the paper of Kinoshita et al. [19] was published, a lot of new experimental data on the R measurement in e^+e^- annihilation into hadrons has been accumulated. Progress in the low energy range was mostly due to experiments at VEPP-2M at Novosibirsk where three groups (OLYA, ND and CMD) provided independently the information on different exclusive channels of e^+e^- annihilation and at DCI at Orsay coming from the DM2 experiment. In the Novosibirsk experiments the center of mass (c.m.) energy range from the threshold of hadron production up to 1.4 GeV was studied, whereas Orsay experiments covered the c.m. energy range from 1.35 up to 2.3 GeV. The high integrated luminosity collected in these experiments allowed them to improve considerably their statistical precision. Larger solid angles of the detectors and the use of electromagnetic calorimeters providing detection of photons with good energy resolution facilitated the identification of the large number of exclusive annihilation channels.

In the Novosibirsk energy range the cross section is dominated by ρ, ω and ϕ resonances, resulting in its strong energy dependence. Typical multiplicities in multi-pion production do not exceed five, making the total number of accessible channels rather small. Besides that, the cross section of the two-body channels is dominating the total cross section. All these circumstances make the usual inclusive procedure of R determi-

[2] The problem addressed in Ref. [52] is that "The best fits to the data which are affected by systematic uncertainties on the normalization factor have the tendency to produce curves lower than expected, if the covariance matrix of the data points is used in the definition of χ^2".

nation from the total number of multi-hadronic events of a different type almost meaningless and subject to large uncertainties. Therefore experimental efforts were aimed at the selection of exclusive channels followed by the "exclusive" R determination by simply adding contributions of different reactions. The energy range from 1.4 up to 2.3 GeV systematically studied by Orsay and Frascati groups is much worse understood. It is clear that higher vector mesons play an important role, but their precise parameters are not yet known, thus making a phenomenological model approach rather ambiguous (see the recent paper [54]). The cross section of multi-hadronic channels is considerably larger than that of two-body channels. However, since the multiplicity and therefore the number of possible annihilation channels is still not too big, the approach can be twofold: studies of exclusive channels can be complemented by the independent "inclusive" R determination. At larger energies (above approximately 2 GeV) data on the cross sections of separate channels are missing, only few exclusive channels have been measured (usually in the near resonance region) and there are "inclusive" R determinations only.

The reaction $e^+e^- \to \pi^+\pi^-$ was studied with high precision by the two groups OLYA and CMD which found good agreement between each other and the results of the joint analysis were published in Ref. [18]. In the CMD experiment 24 points from 360 to 820 MeV have been studied with a systematic uncertainty less than 2%. OLYA performed scanning of the energy region from 640 to 1400 MeV with a small energy step and had a systematic uncertainty from about 4% at the ρ-meson peak up to 15% at 1400 MeV. Also used were the older data near threshold from OLYA [55], TOF [56], NA7 [57] and VEPP-2M [58] as well as the measurements from 483 to 1096 MeV by DM1 [59]. The data are shown in Fig. 3. At higher energies this reaction was systematically studied by DM2 [60]. Older results from $\mu\pi$ [61], BCF [62], and MEA [63] at Frascati are also included in the analysis.

The reaction $e^+e^- \to \pi^+\pi^-\pi^0$ was studied by different Orsay and Novosibirsk groups at the ω and ϕ meson (for these data we used the values of the leptonic widths from the Review of Particle Properties [42] to calculate analytically the resonance contributions) as well as in the off–resonance region by CMD [64], ND [65] at Novosibirsk and M2N [66], M3N [67], DM1 [69], and DM2 [70] at Orsay.

There are two channels in four-pion production: $2\pi^+2\pi^-$ and $\pi^+\pi^-\pi^0\pi^0$. OLYA [71, 72] and ND [65] who scanned the energy region from about 640 to 1400 MeV provided results on both, while CMD [73] measured the cross section of the latter in 9 points from 1019 up to 1403 MeV. The values of the cross section determined by ND are usually higher than those of OLYA in both reaction channels; however, they are within systematic uncertainties which are estimated by the authors to be 15% and 10% respectively for ND and 20% in both cases for OLYA. CMD claimed a 10% systematic uncertainty and within it agreed with both ND and OLYA. At higher energies we used the data from M3N [67], MEA [68], DM1 [74] and DM2 [75, 76]. Since we are interested in the values of total cross sections only, the mechanism of particle production is in general not important for our analysis. However, one should note that the reaction $e^+e^- \to \omega\pi^0$ plays an important role in the production of the $\pi^+\pi^-2\pi^0$ final state. Since ω has a 8.5% branching ratio for the $\pi^0\gamma$ decay [42] it should be taken into account separately since it will be missed in the inclusive analysis. Accordingly we add $\sigma_{\omega\pi^0} B(\omega \to \pi^0\gamma)$ to the total cross section, a contribution which was previously ignored.

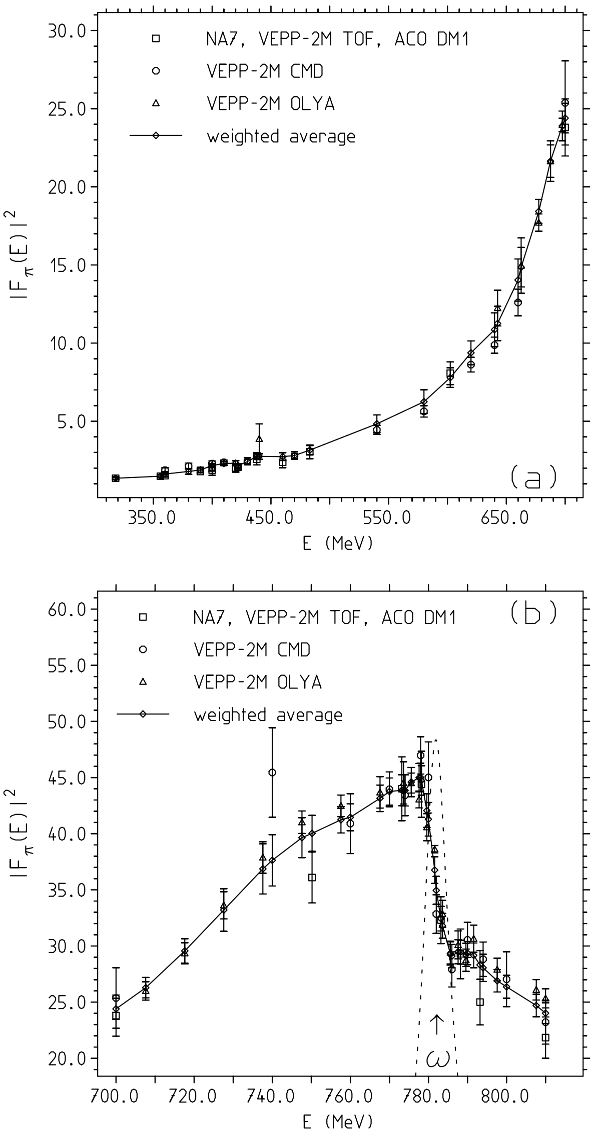

Fig. 3. a,b The pion form factor $|F_\pi(s)|^2$ for 0.32 to 0.81 GeV. In this and the following figures only the statistical error bars are shown

The cross section of the reaction $e^+e^- \to 2\pi^+2\pi^-\pi^0$ was measured at low energy by CMD [73] and at higher energy by different groups. The most precise of them are those by DM1 [77] and DM2 [70]. Its isospin partner $e^+e^- \to \pi^+\pi^-3\pi^0$ is much worse studied, but as mentioned above, the rigorous isotopic symmetry relation requires that its cross section be two times smaller.

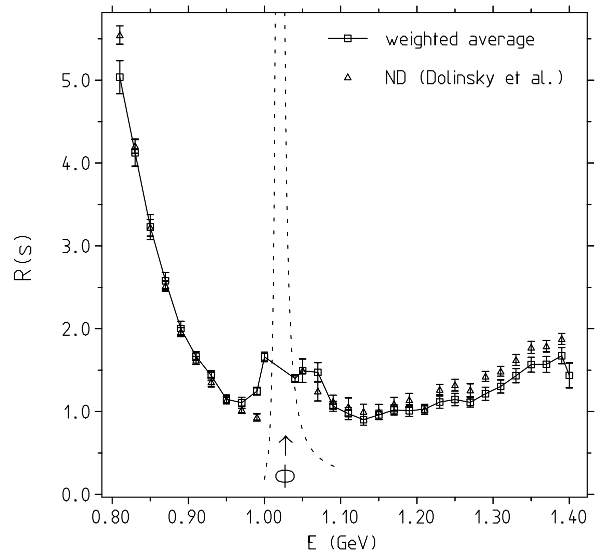

Fig. 4. Averaged value of R for 0.81 to 1.4 GeV calculated from the exclusive channels using all available data. For comparison the R values compiled in Ref. [65] are shown

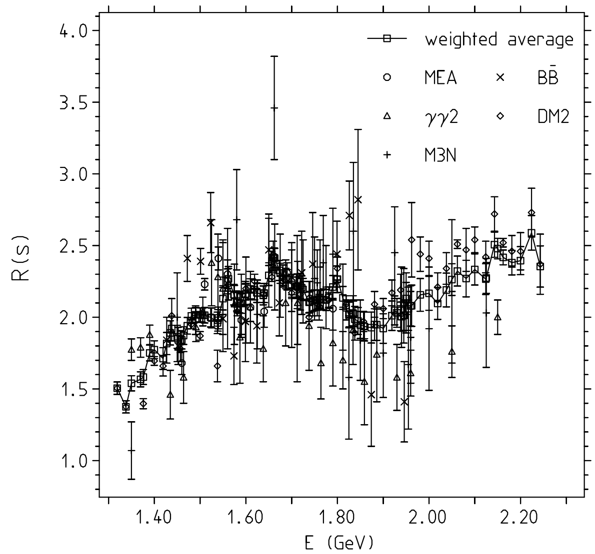

Fig. 5. $R(s)$ in the range 1.4 to 2.3 GeV calculated from the available $R(n>2)$ compilations with the two-body channels added up

Since $\omega\pi\pi$ is a dominant mechanism of five pion production, one should make a correction for it similar to that for the reaction $e^+e^- \to \omega\pi^0$.

Six pion production is much less studied. There are three possible final states of which only $3\pi^+3\pi^-$ and $2\pi^+2\pi^-2\pi^0$ have been observed. The isotopic symmetry does not give unfortunately the rigorous relations between different isotopic partners [78]; however, one can expect that the corrections for the missing parts are small. The existing data are rather controversial. The $\gamma\gamma2$ [79] measurements are typically characterized by much higher values of the cross section hardly compatible with the measurements of DM1 [80] and DM2 [75]. Measurements at low energy are also available from CMD [73].

The reaction $e^+e^- \to \eta\pi^+\pi^-$ was studied by [81] and [82].

Production of kaon pairs was studied by OLYA [83, 84], CMD [85], DM1 [86] and DM2 [88].

DM1 [89] and DM2 [75] measured also cross sections of the reactions $e^+e^- \to K\bar{K}\pi$ and $K\bar{K}\pi\pi$. However, not all possible combinations have been studied. The corrections for the missing modes should be applied.

Information on the production of baryons is scarce. Measurements by DM1 [90], DM2 [91] and FENICE [92] showed that the cross section is small. However, it should be taken into account if R is determined inclusively.

Our compilation of R, obtained following the procedure described in Sec. 4.3., is shown in Figs. 4 to 8, together with original compilations by the experimental groups themselves. It should be mentioned that part of the large systematic errors given by experiments in particular below the J/ψ are supposed to account for the lack of understanding or performing the radiative corrections. Most experiments have applied radiative corrections including at least the vacuum polarization contribution from the electron, which is the dominant contribution at low energies [35, 37, 38]. The hadronic contribution to the vacuum polarization has been known since the work of Berends and Komen [31] in 1976 but usually it was not included in the QED corrections. We shall assume that on the average experiments have subtracted only the electron contribution to the vacuum polarization and accordingly rescale the R-values by $(1+2\Delta\alpha_e)(\alpha/\alpha(s))^2$ below the J/ψ. As we mentioned before this remark applies to the ω and ϕ resonances as well.

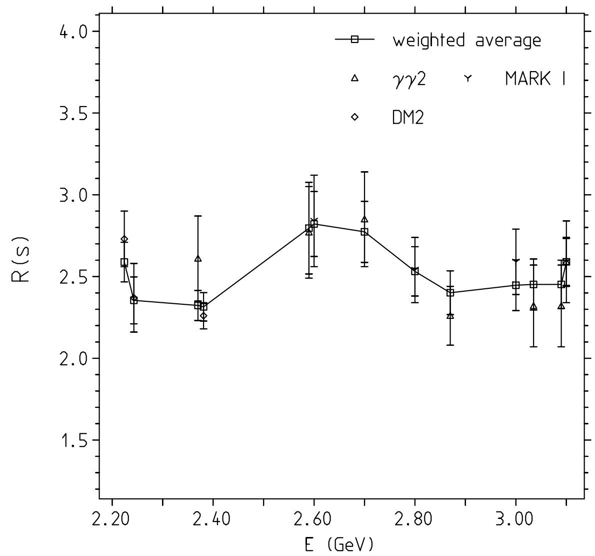

Fig. 6. The R data from the various experiments in the energy range 2.2 to 3.1 GeV

In the high energy region we distinguish the J/ψ and the Υ resonances and the background inclusive measurements of the total hadronic cross section which is usually

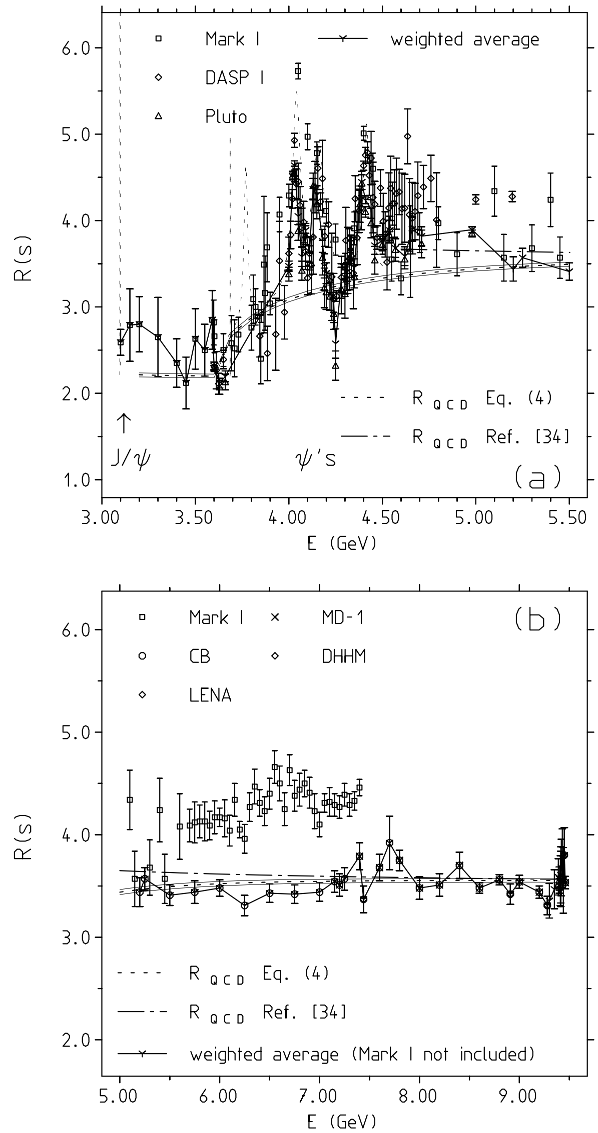

Fig. 7. a,b The R data from the various experiments in the energy range 3.1 to 9.6 GeV. The "weighted mean" does not include the Mark I data above 3.6 GeV. The two perturbation theory results are the $O(\alpha_s^3)$ predictions Eq. (4) and Ref. [34] with the LEP value $\alpha_s(M_Z^2) = 0.126 \pm 0.005$ as input

presented in terms of R-values. The resonance contributions are taken into account as explained in Sec. 4.1. Masses, widths and the electronic branching fractions are taken from the Review of Particle Properties [42]. Since only total errors are given for these quantities, we treat the error from the mass (negligible) and width quadratically and the one from the branching fraction linearly within a family. In this way we take into account that the systematic errors should be added linearly.

In the region from the J/ψ to the Υ R-measurements are available from Mark I [96, 97], DASP [98], PLUTO [99], LENA [100], Crystal Ball (CB) [101] and MD-1 [102] (see Fig. 7). The Crystal Ball Collaboration has carefully reanalyzed their old data and obtained $R(s)$ values substantially lower than Mark I and in agreement with

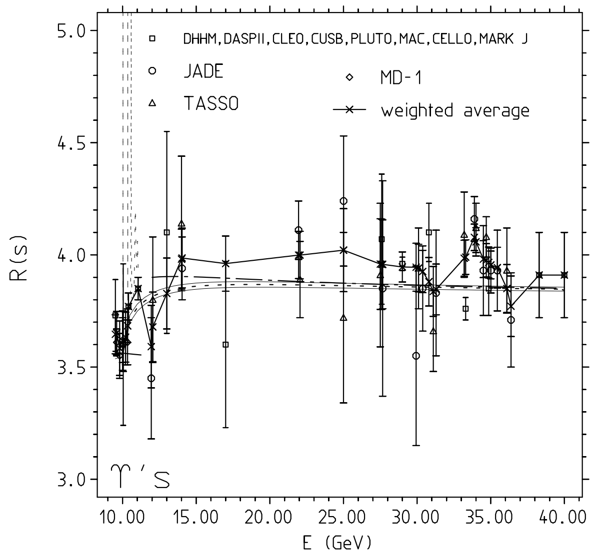

Fig. 8. The R data from the various experiments in the energy range 9.6 to 40 GeV. The two perturbation theory results are the $O(\alpha_s^3)$ predictions Eq. (4) (dotted line) and Ref. [34] (dash-dot line) with the LEP value $\alpha_s(M_Z^2) = 0.126 \pm 0.005$ as input

the other experiments PLUTO, LENA and MD-1. The results are now much closer to expectations from perturbative QCD ($R \sim 10/3$ at lowest order). The change of the data is mainly due to a up-to-date treatment of the QED radiative corrections and τ subtraction. Ref. [101] gives a detailed description of how precisely the radiative corrections have been performed. The procedure is based on the calculation of Ref. [37] which has been applied by all DESY experiments. Thus, except from the Mark I data, all data above the J/ψ resonance have published properly normalized R–values. The Mark I values we rescale by $(1 + 2\Delta\alpha_l)(\alpha/\alpha(s))^2$, because we assume that hadronic vacuum polarization effects have not been subtracted, while the leptonic correction has been taken into account in a non-resummed form.

Below we will study the option of including and discarding the Mark I data in the overlapping range, where the Mark I data systematically lie 28% higher as we can see in Fig. 7.

Above the Υ we include PETRA and PEP data up to $E_{\rm cut} = 40$ GeV. In this range we correct for the $\gamma - Z$ mixing contribution as described earlier. For larger energies the $\gamma - Z$ mixing would be substantial and make the analysis less transparent. In fact perturbative QCD is reliable for evaluating the high energy contribution already at lower energies. In the PETRA/PEP range there are many measurements of rather high accuracy available, a fact which is particularly important for the precise determination of $\alpha(M_Z)$. Data are mainly from CELLO [103], JADE [104], MARK J [105] and TASSO [106]. Further included are the R-measurements from DASP [98], DHHM [107], CLEO [108], CUSB [109], HRS [110], MAC [111] and MD-1 [102](see Fig. 8).

Table 3. Contributions to $a_\mu^{\mathrm{had}} \times 10^{10}$

final state	energy range (GeV)	contribution (stat) (syst)	rel. err.	abs. err.
ρ	(0.28, 0.81)	426.66 (5.61) (10.62)	2.8%	1.7%
ω	(0.42, 0.81)	37.76 (0.45) (1.02)	3.0%	0.2%
ϕ	(1.00, 1.04)	38.55 (0.54) (0.89)	2.7%	0.1%
J/ψ		8.60 (0.41) (0.40)	6.7%	0.1%
Υ		0.10 (0.00) (0.01)	6.7%	0.0%
hadrons	(0.81, 1.40)	112.85 (1.33) (5.49)	5.0%	0.8%
hadrons	(1.40, 3.10)	56.43 (0.45) (7.22)	12.8%	1.0%
hadrons	(3.10, 3.60)	4.47 (0.23) (0.86)	19.9%	0.1%
hadrons	(3.60, 9.46)	14.06 (0.07) (0.90)	6.5%	0.1%
hadrons	(9.46, 40.0)	2.70 (0.03) (0.13)	4.9%	0.0%
perturbative	(40.0, ∞)	0.16 (0.00) (0.00)	0.2%	0.0%
total		702.35 (5.85) (14.09)	2.2 %	2.2%

Table 4. ρ–contributions to $a_\mu^{\mathrm{had}} \times 10^{10}$ of different experiments

Energy range:	(0.32, 0.36) GeV	(0.36, 0.40) GeV	(0.40, 0.81) GeV
DM1$^+$	6.213 (0.372)(0.214)	9.225 (0.432)(0.197)	409.739(14.450)(9.331)
CMD	–	11.533 (0.710)(0.231)	414.176(11.051)(8.284)
OLYA	–	–	472.399(24.364)(22.672)
Averaged	6.213 (0.372)(0.214)	9.890 (0.373)(0.146)	418.120(9.939)(7.661)
Tab. 3	6.177 (0.370)(0.210)	9.363 (0.582)(0.269)	409.034(5.572)(10.136)

6. Results

The results presented here have been obtained following the procedure described in Sec. 4.3. For the $\pi^+\pi^-$ data we have three sets of data points as collected in Ref. [18]. They are displayed in Fig. 3 and we label them by DM1$^+$ (which includes data from DM1, NA7 and TOF), CMD and OLYA. In the range 0.81-1.4 GeV we use a compilation similar to the one in Ref. [65] but with all available data which are shown in Fig. 4. This is done by adding up the individual channels, where for each channel weighted averages are taken as described in Sec.4.3. The ϕ-resonance is taken into account in analytic form in the narrow interval between 1.00 and 1.04 GeV. Outside this interval the ϕ contribution is included in the background. The cut at 1.4 GeV is justified as it is the energy limit of VEPP-2M. From 1.4 to 2.3 GeV we combine R–values published by the experiments MEA, $\gamma\gamma2$, $\mathrm{B\bar{B}}$, M3N, DM1 and DM2; from 2.3 to 3.1 GeV data collected by $\gamma\gamma2$, DM2 and Mark I are available, where the last two give R while the others $R(n>2)$, in which case the 2-body channels have to be taken into account separately. In taking weighted averages here we did not account yet for the fact that some measurements have been performed at the same machine and hence have common normalization errors. We therefore enlarge the systematic error in this domain by a factor $\sqrt{2}$ to be on the conservative side. The data for this region are shown in Figs. 5 and 6. In the region between the J/ψ and Υ resonances we again compare two methods. First we combine data by calculating the weighted averages as described above. The Mark I data are treated as an independent set, and are eventually combined after integration. Alternatively, we split the region in such a way that results from different experiments can be combined after integration. From 3.1 to 3.6 GeV we have data from Mark I, form 3.6 to 5.2 GeV Mark I, DASP and PLUTO, from 5.2 to 7.2 GeV Mark I, CB and PLUTO and from 7.2 to 9.46 GeV PLUTO and MD-1. Here we take weighted averages after integration. The different energy ranges mentioned are treated as independent when adding up the results, a procedure which again may not be fully justified.

The data above the J/ψ still include the resonance contributions $\psi(4040)$, $\psi(4160)$ and $\psi(4415)$, which we subtract and include in the J/ψ–family resonance contribution. Finally from the Υ to 40 GeV we take weighted averages for the data sets JADE, TASSO, MD-1 and others as shown in Fig. 8. Consistent results are obtained if we combine the data pointwise and add all systematic errors linearly. The results for a_μ^{had} are presented in Tab. 3. The last two columns give the relative uncertainty (rel.err.) of the individual contribution and the absolute uncertainty (abs.err.) relative to the total result. The ρ-contribution always includes a contribution 2.08 (0.01)(0.05) calculated using chiral perturbation theory from the 2π-threshold to 318 MeV where data points start. For details we refer to Sec. 4.2. In spite of a major effort in the ρ region the result is almost the same as the one obtained using Kinoshita's fit [19] which was used subsequently in [22, 25, 27, 28]. A previous analysis [22] gave the results 428.95(1.71)(12.81)[426.68(1.70)(12.74)] for the ρ contribution in the range (0.28, 0.81) GeV and 125.54(3.89)(11.61)[124.27(3.83)(11.46)] for the range (0.81,1.40) GeV. The values in square brackets are the ones obtained after correcting for the missing subtraction of the hadronic vacuum polarization. While the ρ contribution below 0.81 GeV remains unchanged the ρ–tail plus background up to 1.4 GeV turns out to be somewhat smaller.

If we would treat the different experiments separately and then take weighted averages in common domains we would obtain 436.30(9.95)(8.02) for the ρ up to 0.81 GeV, a somewhat higher value. Details are illustrated by Tab. 4. The high value is the result of a failure of the trapezoidal rule when applied to the OLYA data. The reason is that the three lowest points have much larger energy separations than the other points at higher energies and a high weight due to the $1/s^2$ behavior of the kernel. Therefore the first three points yield a large contribution to the integral. Actually, applying the trapezoidal rule here we overestimate the contribution because the low energy tail of the resonance is a strongly varying concave function. This problem is largely circumvented by combining data from different experiments before integration. Note that, while the integrals taken over the whole range agree quite well between different experiments, the individual contributions in the subdomains do not agree within errors. Apparently the integral is better defined than the local values. In other words, the $\rho \to \pi\pi$ region is after all not as well established as the experiments claim. There are many points where the weighted average yields $S > 1$ and the error must be enlarged.

If we just take the collection of all points in a given energy region and add systematic errors linearly we obtain 413.80(8.10)(23.81) for the range up to 0.81 GeV, with a much larger systematic error. Similarly, we find 113.71(1.31)(12.31) for the contribution from 0.81 to 1.40 GeV. The final result would be 695.42(8.30)(27.52). We remind the reader that in the important region from 0.81 to 1.4 GeV data for the channels $\pi^+\pi^-2\pi^0$ and $\pi^+\pi^-\pi^+\pi^-$ from ND lie substantially higher than from other experiments as can be seen in Fig. 4. A new experiment is required to resolve the current discrepancy.

In Tab. 5 we give the results we obtain when using the resummed photon propagator in the diagram Fig. 1. This dressed contribution we denote by $a_\mu^{\mathrm{had}\,*}$. We notice that the difference between the dressed and the undressed form is about 23, slightly larger than the uncertainty of 16 and of the same size as the interesting weak contribution $a_\mu^{\mathrm{weak}} \simeq 20$. For a_τ the results are collected in Tab. 6 (see also the last reference of Ref.[17] and [23]). The hadronic contribution to the electron anomaly is $a_e^{\mathrm{had}\,*} = (194.48 \pm 1.69 \pm 3.87) \times 10^{-14}$.

We now turn to the hadronic contribution to the shift in the fine structure constant. In Tab. 7 we list the contributions from different energy ranges.

The resonance contributions were evaluated as discussed in Sec. 4.1. Note that Breit-Wigner resonances may be treated non-relativistically, relativistically and with different off-resonance behavior. Results obtained for different resonance shapes are listed in Tab. 8. We note that the narrow width approximation gives generally larger values than the Breit-Wigner parametrizations in either the non-relativistic form, the relativistic form with constant width or the relativistic form with s-dependent width. As expected, the deviations obtained from using different types of Breit-Wigner parametrizations are within the experimental uncertainties.

The region between the J/ψ and the Υ has been split into two subdomains. From the J/ψ to 3.6 GeV only Mark I data are available. Above 3.6 GeV up to the Υ one may think about skipping the Mark I data, as mentioned before. Because of the resonances included in the data we integrate the PLUTO, DASP and Mark I data separately in the region from 3.6 to 5.2 GeV and combine the results after integration.

The analysis shows that the results are affected in a minor way if we include the Mark I data. Taking the weighted average of the two values obtained from the Mark I data on the one hand and the other data on the other hand we find 50.79(0.20)(3.20). If we combine results from individual experiments and take weighted av-

Table 5. Contributions to $a_\mu^{\mathrm{had}\,*} \times 10^{10}$

final state	energy range (GeV)	contrib. (stat) (syst)
ρ	(0.28, 0.81)	438.63 (5.76) (10.91)
ω	(0.42, 0.81)	38.90 (0.47) (1.05)
ϕ	(1.00, 1.04)	39.86 (0.56) (0.92)
J/ψ		9.05 (0.43) (0.42)
Υ		0.11 (0.00) (0.01)
hadrons	(0.81, 1.40)	116.84 (1.38) (5.69)
hadrons	(1.40, 3.10)	58.92 (0.47) (7.55)
hadrons	(3.10, 3.60)	4.71 (0.25) (0.90)
hadrons	(3.60, 9.46)	14.91 (0.08) (0.96)
hadrons	(9.46, 40.0)	2.94 (0.03) (0.14)
perturbative	(40.0, ∞)	0.18 (0.00) (0.00)
total		725.04 (6.01) (14.57)

Table 6. Contributions to $a_\tau^{\mathrm{had}\,*} \times 10^{8}$

final state	energy range (GeV)	contrib. (stat) (syst)
ρ	(0.28, 0.81)	141.35 (1.66) (3.42)
ω	(0.42, 0.81)	15.06 (0.18) (0.41)
ϕ	(1.00, 1.04)	21.06 (0.29) (0.48)
J/ψ		13.47 (0.64) (0.65)
Υ		0.26 (0.01) (0.01)
hadrons	(0.81, 1.40)	58.23 (0.64) (3.11)
hadrons	(1.40, 3.10)	58.84 (0.56) (7.94)
hadrons	(3.10, 3.60)	7.02 (0.36) (1.35)
hadrons	(3.60, 9.46)	28.04 (0.14) (1.80)
hadrons	(9.46, 40.0)	7.36 (0.07) (0.35)
perturbative	(40.0, ∞)	0.50 (0.00) (0.00)
total		351.18 (2.04) (9.51)

Table 7. Contributions to $\Delta\alpha_{\rm had}^{(5)} \times 10^4$

final state	energy range (GeV)	contribution (stat) (syst)	Ref. [28]
ρ	(0.28, 0.81)	26.08[26.23] (0.29) (0.62)	26.07(0.10)(0.78)
ω	(0.42, 0.81)	2.93[2.96] (0.04) (0.08)	3.43(0.35)(0.10)
ϕ	(1.00, 1.04)	5.08[5.15] (0.07) (0.12)	5.27(0.24)(0.16)
J/ψ		11.34[11.93] (0.55) (0.61)	10.16(1.34)(1.52)
Υ		1.18[1.27] (0.05) (0.06)	1.17(0.04)(0.07)
hadrons	(0.81, 1.40)	13.83[13.99] (0.15) (0.79)	15.63(0.68)(1.73)
hadrons	(1.40, 3.10)	27.62[28.23] (0.32) (4.01)	27.95(0.60)(5.59)
hadrons	(3.10, 3.60)	5.82[5.98] (0.30) (1.12)	5.98(0.31)(1.15)
hadrons	(3.60, 9.46)	50.60[50.50] (0.24) (3.33)	50.27(0.51)(3.14)
hadrons	(9.46, 40.0)	93.07 (0.86) (3.39)	93.60(1.24)(2.91)
perturbative	(40.0, ∞)	42.82 (0.00) (0.10)	42.67(0.29)(0.59)
total		280.37[282.13](1.18) (6.43)	282.21(2.19)(8.30)

Table 8. Shape dependence of resonance contributions

state	range (GeV)	a)	b)	c)	d)
ω	(0.42, 0.81)	3.138	2.994	2.952	2.931
ϕ	(1.00, 1.04)	5.451	5.068	5.069	5.083
J/ψ		11.380	11.342	11.338	11.338
Υ		1.182	1.178	1.178	1.178

a) narrow width approximation

b) non-relativistic

c) relativistic constant width

d) relativistic s-dependent width

erages for overlapping domains we get 50.69[51.20] (0.30) (2.74) if we exclude [include] the Mark I data. These checks show that the trapezoidal rule works consistently and there is no serious problem of properly weighting the data from different experiments according to their uncertainties[3]. The values obtained compare with the ones from a previous analysis [28] and are all found to be consistent.

We have checked the non-resonant part above the J/ψ, which contributes a major part to $\Delta\alpha$, against the 3-loop perturbative QCD prediction, using the LEP value $\alpha_s(M_Z^2) = 0.126 \pm 0.005$ [24] for the strong interaction constant as an input. We obtain

Range	Data	Ref. [34]	Eq. (4)
$5.00-9.46$ GeV	32.63	35.78	34.97
$12.0-40.0$ GeV	79.22	78.23	77.64

The two QCD results differ by a different treatment of mass effects. In Eq. (4) just the lowest order threshold factor is used, while Ref. [34] also takes into account charm and bottom mass effects in the higher order terms in an expansion in m^2/s.

We have also varied the high energy cut energy from $E_{\rm cut}$=40 to 30, 20 and 12 GeV and found stable results: 0.0280 ± 0.0007, 0.0280 ± 0.0006, 0.0280 ± 0.0006 and 0.0279 ± 0.0006. We note that data and the perturbative prediction in average fit fairly well above the resonance regions, as may be seen in Figs. 7 and 8. In addition we observe that the onset of the $\gamma - Z$ mixing is well under control after the subtraction of the $\gamma - Z$ interference term which we described at the end of Sec. 3. This subtraction was applied already in previous work [27, 28]. Doubtless, the LEP experiments have dramatically improved our confidence in perturbative QCD and we may well use a much lower $E_{\rm cut}$, such as for example 12 GeV, and use perturbative QCD also in the range from e.g. 5 GeV, up to the Υ threshold. As a result we find 0.0282 ± 0.0005 and hence a slightly larger result with a smaller error. However, if we move the cut slightly from 5 GeV to 4.5 GeV we obtain 0.0280 ± 0.0005 which shows that the better accuracy is delusive as the central value depends substantially on the cut[4]. A glance at Fig. 7a shows that the PLUTO data points in the region of the $\psi(4040)$, $\psi(4160)$ and $\psi(4415)$ resonances are lower than "perturbative QCD plus the Breit-Wigner

[3] This is in contrast to claims in Ref. [29] that the trapezoidal rule does not allow us to combine data from different experiments in a reasonable way and automatically has the effect of weighting all inputs equally. Note that in previous analysis [25, 27, 28] properly weighted averages of data from different experiments were used unless data from different experiments had very similar errors in which case they were treated like points from one experiment. As systematic errors for a given "experiment" are added linearly the simplified treatment of equal weighting of data has primarily the effect of yielding a too conservative estimate for the systematic error. In Ref. [29] data are fitted to smooth functions before integration and systematically lower results are obtained (see also the discussion in Ref [52]). The author of Ref. [29] believes more in integration of his fits than in trapezoidal integration, without giving any actual arguments; moreover he does not mention the fact that his fitting method has to rely on some rather arbitrary assumptions about the sources of systematic effects and/or correlations.

[4] Our findings do not confirm those of Ref. [30]. These authors essentially use perturbative QCD with the world average strong coupling $\alpha_s = 0.118 \pm 0.007$ for $E > 3$ GeV, plus the resonances, instead of the data. Data, in so far as they are used, are rescaled to meet the result of perturbation theory. Their results lie systematically lower than ours. The third order QCD prediction is assumed to be exact down to 3 GeV.

resonances". Note that the resonances depicted in Fig. 7a have been scaled down by $(\alpha/\alpha(s))^2$ in order to have the proper normalization for R. If one applies the missing $(1+2\Delta\alpha_l)(\alpha/\alpha(s))^2$ correction to the Mark I data they agree much better than the PLUTO data with the above "prediction".

As a main result we obtain

$$\Delta\alpha^{(5)}_{\mathrm{had}} = 0.0280[0.0282] \pm 0.0007 \tag{21}$$

for $M_Z = 91.1888$ GeV consistent with the 1991 update [28]. In brackets we also give the value without any $(\alpha/\alpha(s))^2$ rescaling of data. These results confirm the assumption made in previous work, namely, that corrections which account for the missing subtractions of the vacuum polarization contributions are small and well within errors. In fact usually the "missing corrections" were estimated and included as a part of the systematic error. This small correction was not taken into account in [28].

A lower central value than in [25, 27] is mainly due to the new more precise data from CB [101] and MD-1 [102]. The Mark I data dominated in most of the earlier estimates. The replacement of the Mark I data by the CB data in the common energy range has been presented in the update [28] some time ago. Undressing of the resonance contributions and some supplementary subtractions of hadronic vacuum polarization contributions lead to a correction of -0.000176. We now employ the value for α_s from LEP. In Refs. [25, 27, 28] the α_s value used was the one obtained by the PEP/PETRA experiments.

The uncertainty obtained in this analysis is smaller mainly for the following reasons. First, we are using more complete data in the range from 0.81 to 3.1 GeV. In particular the DM2 data [75] in the range from 1.35 to 2.3 GeV, which have smaller uncertainties, were not used in previous estimates. Second, previously in [27, 28] an overall 20% systematic error was assumed in this range, which corresponded to a typical systematic error reported by the individual experiments. Furthermore, in these references, a conservative 3.5% error, which was the accuracy of the PEP/PETRA data, was assumed for the perturbative tail. This more conservative treatment of errors in Ref. [27] lead to an increase to 0.0009 from 0.0007 which was previously obtained in Ref. [25]. The more complete collection of data allows us to better justify the more precise result now. Although the replacement of the Mark I data by the CB data helps in reducing the uncertainty it is not the main reason as can be checked in Tab. 7. The higher accuracy of the resonance parameters also helped in reducing the uncertainty.

We finally summarize in Tab. 9 the uncertainties obtained for the different contributions.

The last line $(\star)$ of Tab. 9 gives the uncertainty one would get if the experimental errors on $R(s)$ would be reduced to 5% in all the regions which exhibit uncertainties larger than that. The last column gives the uncertainty relative to the total result. The table clearly tells us that the background contributions require a new scan for all energies up to about 12 GeV. For higher energies one may rely more on perturbative QCD. It seems unlikely

Table 9. "Distribution" of uncertainties

	$\Delta\alpha^{(5)}_{\mathrm{had}} \times 10^4$	rel. err.	abs.err.
Resonances:	46.61 (1.08)	2.3 %	0.4 %
Background:			
$E < M_{J/\psi}$	41.45 (4.11)	9.9 %	1.5 %
$M_{J/\psi} < E < 3.6$ GeV	5.82 (1.16)	19.9 %	0.4 %
3.6 GeV $< E < M_\Upsilon$	50.60 (3.34)	6.6 %	1.2 %
$M_\Upsilon < E < 40$ GeV	93.07 (3.50)	3.8 %	1.2 %
$E < 40$ GeV data	237.55 (6.54)	2.8 %	2.3 %
40 GeV $< E$ QCD	42.82 (0.10)	0.2 %	0.0 %
total	280.37 (6.54)	2.3 %	
$(\star)$	(4.92)	(1.8 %)	

that a substantial improvement will be possible in the foreseeable future. Physics will need a global update of many experiments in order to be prepared for the next level of precision physics.

7. Summary and outlook

The question at the beginning of this investigation was whether one could improve the previous estimates in the present situation and how things could develop in future. While there has been very little truly new experimental results, some groups have published updated results which were available before as preliminary data only. Examples are the ND results [65], the DM2 results [70, 75, 76, 91] and the Crystal Ball results [101], where the latter have already been used in [28]. New results from VEPP-4 [102] have been included as well. In addition we have made an effort to collect as much as possible all the available data. It should be noted that for example the Durham-RAL High Energy Physics database utilized in Ref. [30] is incomplete and in many cases contains preliminary data only while the final results are missing. In our analysis we also used data which have not yet been included in the collection [112] of e^+e^- data which was published recently. Another issue was to check what corrections were applied to the published data, which required a careful reading of the original papers.

Additional motivations for performing this update were the following: the recent issues of the Review of Particle Properties [42] had some improvements on the resonance parameters and there was progress in calculating $R(s)$ at high energies in perturbative QCD [33, 34, 24]. For the muon anomaly the study of the low energy end by means of chiral perturbation theory [49] allowed us to reduce potential model-dependences of earlier approaches.

That all these efforts mentioned lead to minor changes of the results was to be expected. Nevertheless we think such an update was necessary and it will not be soon that a more precise estimate will be possible.

Refinements and improvements were proposed recently in Refs. [29] and [30]. More theoretical attempts to calculate the photon vacuum polarization may be found in [113, 114, 115, 116, 117] to mention only a few. We all know about the difficulties to make accurate *reliable* predictions in strong interaction physics. Here we have tried to estimate hadronic vacuum polarization effects in a model-independent way exploiting as much as possible the existing data, and we find results consistent with known estimates.

For the muon anomaly we propose to use the RG improved value which is 1σ higher than the bare one usually considered. With our value for $a_\mu^{\mathrm{had}\,*}$, and assuming that the subleading hadronic contributions and their uncertainties are as given by Kinoshita et al. [19], we obtain

$$a_\mu^{\mathrm{the}} = (11659210 \pm 16) \times 10^{-10}$$

and therefore at present we have

$$a_\mu^{\mathrm{exp}} - a_\mu^{\mathrm{the}} = (20 \pm 86) \times 10^{-10} \; .$$

The forthcoming Brookhaven experiment is expected to reduce this uncertainty to $\pm 17 \times 10^{-10}$. Recently there is an ongoing discussion about the true size of the hadronic light–by–light scattering contribution [32] and therefore the value and the uncertainty of the theoretical prediction still may change.

Finally, by adding the hadronic contribution, the leptonic contribution $\Delta\alpha_l = 0.031421$ and a top contribution $\Delta\alpha_{\mathrm{top}} = -0.000061$ (obtained by integrating Eq. (4) with running parameters numerically) we find the total shift by the fermions[5]

$$\Delta\alpha = 0.05940 \pm 0.00065$$

and hence for the effective fine structure constant

$$\alpha(M_Z^2)^{-1} = 128.896 \pm 0.090 \quad .$$

What about the future? Progress in decreasing the hadronic uncertainties can be expected from the experiments at the general purpose CMD-2 detector at the Novosibirsk VEPP-2M collider, which has an ambitious goal of measuring $\sigma_{\mathrm{tot}}(e^+e^- \to \mathrm{hadrons})$ with an accuracy better than 1%. The experiment is in progress and during the 1995 runs it is planned to study the energy range from the threshold of two pion production up to the ϕ meson with a 10 MeV step and achieve a statistical accuracy of 3% in each point [119]. Further work will be needed to understand the detector performance as well as low energy radiative corrections at such a level that systematic uncertainties will be understood with the desired accuracy. After that the energy range from the ϕ meson up to the maximum attainable energy of 1.4 GeV will be studied. Here, as discussed above, additional difficulties can arise for the high precision cross section measurements because of the intermediate mechanism uncertainty. Let us assume that a systematic uncertainty of 1% will be achieved for the ρ, ω and ϕ mesons and that of 2% for the hadron continuum between 0.81 and 1.40 GeV. The statistical error in the integrals can be neglected and a resulting systematic uncertainty in the muon anomaly decreases from 15×10^{-10} to 9×10^{-10} of which 8×10^{-10} come from the contribution of the hadron continuum between 1.4 and 3.1 GeV.

[5] We do not include the W boson contribution here because it is gauge dependent, and splitting off a gauge invariant part and combining the reminder with the photon vertex is not unique [118].

Further progress can be expected from the future generation experiments at DAΦNE at Frascati and the upgraded VEPP-2M. Plans at DAΦNE are to perform a scan with 100 values from 0.28 to 1.5 GeV c.m. energy with a precision which will allow to reduce the uncertainty from the hadronic vacuum polarization contribution to a_μ to about 0.3% [120]. This will reduce the uncertainty for the region below 1.4 GeV to 1.5×10^{-10} and the remaining total hadronic vacuum polarization uncertainty in the prediction of a_μ would be 8×10^{-10}, which again is completely dominated by the contribution from 1.4 to 3.1 GeV. The DAΦNE measurement will be possible earliest by end of 1997 but then can be done within a few days. Obviously, the VEPP-2M and the DAΦNE measurements will be crucial for the physics we will be able to learn from the planned Brookhaven Experiment 821 [12].

No improvement is in sight at higher energies. The energy region from 1.4 to 3.1 GeV and in addition that of higher energies from 3.1 up to about 12 to 40 GeV, depending on how much one is accepting to rely on perturbative QCD, will give a dominant contribution to the uncertainty of the fine structure constant shift.

One can conclude that a real breakthrough in improving the precision of the hadronic vacuum polarization will require dedicated efforts in high precision R-measurements in a wide energy range.

Acknowledgement. One of the authors (S.E) would like to thank the Paul Scherrer Institute where part of this work was done for its hospitality, and Boris Khazin, Georgi Shestakov and Boris Shwartz for useful discussions. We also thank Rinaldo Baldini for providing us sets of R–data and Paula Franzini for helpful discussions and for carefully reading the manuscript.

Appendix: "Dressed" versus "undressed" quantities

Equations (1) and (11) can be derived from the convergent dispersion relation

$$\begin{aligned} \mathrm{Re}\, \Delta\hat{\Pi}'_\gamma(s) &= \mathrm{Re}\, \hat{\Pi}'_\gamma(s) - \hat{\Pi}'_\gamma(0) \\ &= \frac{s}{\pi}\, \mathrm{Re} \int_{s_0}^{\infty} ds' \frac{\mathrm{Im}\, \hat{\Pi}'_\gamma(s')}{s'(s'-s-\mathrm{i}\varepsilon)} \end{aligned}$$

where $\hat{\Pi}'_\gamma$ is the transversal part of the current-current matrix element of the conserved electromagnetic current

$$\begin{aligned} \hat{\Pi}_{\mu\nu}(q) &= i \int d^4x\, e^{iqx} \;\; < 0|\, T^*\, j_\mu^\gamma(x)\, j_\nu^\gamma(0)\, |0 > \\ &= (q^2 g_{\mu\nu} - q_\mu q_\nu)\hat{\Pi}'_\gamma(q^2) \quad . \end{aligned}$$

This self-energy function exists in the limit where the electromagnetic interaction is switched off and for the hadronic current, in principle, it is determined by QCD. The *irreducible* photon self-energy is given by $\Pi'_\gamma(s) = e^2\hat{\Pi}'_\gamma(s)$. It is well known that the running of $\alpha = e^2/4\pi$ (see Sec. 3) may be understood as a consequence of the Dyson summation of the irreducible photon self-energy

$$\frac{e^2}{s}\ \left(1+\mathrm{Re}\ \Delta\Pi'_\gamma(s)\right) \rightarrow \frac{e^2}{s}\ \mathrm{Re}\ \frac{1}{1-\Delta\Pi'_\gamma(s)} \equiv \frac{e^2(s)}{s}$$

which is equivalent to a RG improvement of the perturbation expansion. For the full photon propagator we have

$$\mathrm{Re}\ \frac{1}{1-\Delta\Pi'_\gamma(s)} = \frac{1}{1-\mathrm{Re}\ \Delta\Pi'_\gamma(s)}\frac{1}{1+(\frac{\mathrm{Im}\ \Pi'_\gamma(s)}{1-\mathrm{Re}\ \Delta\Pi'_\gamma(s)})^2}$$
$$\simeq \frac{1}{1-\mathrm{Re}\ \Delta\Pi'_\gamma(s)} = \frac{e^2(s)}{e^2}$$

for the real part and

$$\mathrm{Im}\ \frac{1}{1-\Delta\Pi'_\gamma(s)} = \frac{\mathrm{Im}\Pi'_\gamma(s)}{(1-\mathrm{Re}\ \Delta\Pi'_\gamma(s))^2}\frac{1}{1+(\frac{\mathrm{Im}\ \Pi'_\gamma(s)}{1-\mathrm{Re}\ \Delta\Pi'_\gamma(s)})^2}$$
$$\simeq \mathrm{Im}\ \Pi'_\gamma(s)\frac{e^4(s)}{e^4}$$

for the imaginary part.

These relations show that in the dispersion relation for the irreducible self-energy one has to use "undressed" (with respect to vacuum polarization effects) quantities and not the physical ones. Thus in the optical theorem (unitarity) one has to use the undressed total cross section

$$-\mathrm{Im}\ \hat{\Pi}'_\gamma(s) = \frac{s}{e^4(s)}\sigma_{\mathrm{had}}(s) = \frac{s}{e^4}\sigma^{(0)}_{\mathrm{had}}(s) = \frac{R(s)}{12\pi}\ .$$

Up to subleading higher order effects the resummed photon propagator may be obtained directly from a dispersion relation by using the dressed physical quantities under the dispersion integral.

References

1. J. Bailey et al. Phys. Lett. 68B (1977) 191; F.J.M. Farley and E. Picasso, Ann. Rev. Nucl. Sci. 29 (1979) 243; in "Quantum Electrodynamics", ed. T. Kinoshita, World Scientific, Singapore, F.J.M. Farley, Z. Phys. C56 (1992) S88.
2. T. Kinoshita, Past, Present and Future of Lepton $g-2$, in Proc. of the 10th Inter. Symposium on "High Energy Spin Physics", Nagoya, Japan, 1992; Z. Phys. C56 (1992) S80; T. Kinoshita, in "Quantum Electrodynamics", ed. T. Kinoshita, World Scientific, Singapore, 1990, pp. 218 - 321.
3. T. Kinoshita and W.B. Lindquist, Phys. Rev. D41 (1990) 593; M.A. Samuel and G. Li, Phys. Rev. D44 (1991) 3935; S. Laporta and E. Remiddi, Phys. Lett. B301 (1993) 440.
4. D.J. Broadhurst, A.L. Kataev and O.V. Tarasov, Phys. Lett. B298 (1993) 445; T. Kinoshita, Phys. Rev. D47 (1993) 5013.
5. T. Kinoshita and W. J. Marciano, in "Quantum Electrodynamics", ed. T. Kinoshita, World Scientific, Singapore, 1990, pp. 419 - 478, and references therein.
6. P. Mery, S.E. Moubarik, M. Perrottet and F.M. Renard, Z. Phys. C46 (1990) 229.
7. W. Bernreuther, Z. Phys. C56 (1992) S97.
8. C. Arzt, M.B. Einhorn and J. Wudka, Phys. Rev. D49 (1994) 1370.
9. M.A. Samuel, G. Li and R. Mendel, Phys. Rev. Lett. 67 (1991) 668.
10. M. Benmerrouche, G. Orlandini and T.G. Steele, Phys. Lett. B316 (1993) 381.
11. L. Vuilleumier, Ph.D. Thesis, University of Lausanne, 1994.
12. B. Lee Roberts (BNL E821), Z. Phys. C56 (1992) S101.
13. C. Bouchiat and L. Michel, J. Phys. Radium 22 (1961) 121.
14. L. Durand, III., Phys. Rev. 128 (1962) 441.
15. M. Gourdin and E. de Rafael, Nucl. Phys. B10 (1969) 667.
16. V. Barger, W.F. Long and M.G. Olsson, Phys. Lett. 60B (1975) 89.
17. J. Calmet, S. Narison, M. Perrottet and E. de Rafael, Phys. Lett. 61B (1976) 283; Rev. Mod. Phys. 49 (1977) 21. S. Narison, J. Phys. G: Nucl. Phys. 4 (1978) 1849.
18. L.M. Barkov et al. (OLYA, CMD), Nucl. Phys. B256 (1985) 365.
19. T. Kinoshita, B. Nižić and Y. Okamata, Phys. Rev. Lett. 52 (1984) 717; Phys. Rev. D31 (1985) 2108.
20. J.A. Casas, C. López and F.J. Ynduráin, Phys. Rev. D32 (1985) 736.
21. Ľ. Martinovič and S. Dubnička, Phys. Rev. D42 (1990) 884.
22. F. Jegerlehner, private communication to V.W. Hughes, 1991.
23. A.Z. Dubničková, S. Dubnička and P. Strizenec, New Evaluation of Hadronic Contributions to the Anomalous Magnetic Moment of Charged Leptons, Dubna-Report, JINR-E2-92-281 (Dec. 1992).
24. D. Schaile (LEP Collaboration), CERN-PPE-94-162, 1994; Talk given at 27th International Conference on High Energy Physics (ICHEP), Glasgow, Scotland, 20-27 July 1994.
25. F. Jegerlehner, Z. Phys. C32 (1986) 195.
26. B. W. Lynn, G. Penso, C. Verzegnassi, Phys. Rev. D35 (1987) 42.
27. H. Burkhardt, F. Jegerlehner, G. Penso, C. Verzegnassi, Z. Phys. C42 (1989) 497.
28. F. Jegerlehner, in "Testing the Standard Model", eds. M. Cvetič, P. Langacker, World Scientific, Singapore, 1991, p. 476; Prog. Part. Nucl. Phys. 27 (1991) 32.
29. M.L. Swartz, Preprint SLAC-PUB-6710, 1994.
30. A.D. Martin and D. Zeppenfeld, Preprint MAD/PH/855, 1994.
31. F.A. Berends and G.J. Komen, Phys. Lett. 63B (1976) 432; E.A. Paschos, Nucl. Phys. B159 (1979) 285; J. Ellis, M.K. Gaillard, D.V. Nanopoulos and S. Rugaz, Nucl. Phys. B176 (1980) 61; W. Wetzel, Z. Phys. C11 (1981) 117.
32. R. Barbieri and E. Remiddi, in "The DAΦNE physics handbook" Vol. II, eds. L. Maiani et al., (INFN, Frascati, 1992) p. 301; M.B. Einhorn, Phys. Rev. D49 (1994) 1668; E. de Rafael, Phys. Lett. B322 (1994) 239.
33. S.G. Gorishny, A.L. Kataev and S.A. Larin, Phys. Lett. B259 (1991) 144; L.R. Surguladze, M.A. Samuel, Phys. Rev. Lett. 66 (1991) 560; idid., 2416(E).
34. K.G. Chetyrkin and J.H. Kühn, Phys. Lett. B342 (1995) 356 and references therein.
35. G. Bonneau and F. Martin, Nucl. Phys. B27 (1971) 381; D.R. Yennie, Phys. Rev. Lett. 34 (1975) 239; J.D. Jackson and D.L. Scharre, Nucl. Instrum. Methods 128 (1975) 13; M. Greco, G. Pancheri-Srivastava and Y. Srivastava, Nucl. Phys. B101 (1975) 234; B202 (1980) 118.
36. Y.S. Tsai, SLAC-PUB-1515 (1975); SLAC-PUB-3129 (1983).
37. F.A. Berends et al., Nucl. Phys. B57 (1973) 381; Nucl. Phys. B68 (1974) 541; F.A. Berends and R. Kleiss, Nucl. Phys. B178 (1981) 141; F.A. Berends, R. Kleiss and S. Jadach, Nucl. Phys. B202 (1982) 63; F.A. Berends and R. Kleiss, Nucl. Phys. B228 (1983) 537.
38. S.I. Eidelman and E.A. Kuraev, Phys. Lett. 80B (1978) 94; V.N. Baier, V.S. Fadin, V.A. Khoze and E.A. Kuraev, Phys. Rep. C78 (1981) 293; E.A. Kuraev and V.S. Fadin, Sov. J. Nucl. Phys. 41 (1985) 466.
39. F.A. Berends and A. Böhm, in "High Energy Electron-Positron Physics", eds. A. Ali and P. Söding, World Scientific, Singapore, 1988, p. 27-140 (see Fig. 8.5).
40. N. Cabbibo and R. Gatto, Phys. Rev. Lett. 4 (1960) 313, Phys. Rev. 124 (1961) 1577.

41. G. Gounaris, J. Sakurai, Phys. Rev. Lett. 21 (1968) 244; M. Gourdin et al., Phys. Lett. 30B (1969) 347; A. Quenzer et al., Phys. Lett. 76B (1978) 512.
42. L. Montanet et al. (Review of Particle Properties), Phys. Rev. D50 (1994) p.1, 1173.
43. G.P. Yost et al. (Review of Particle Properties), Phys. Lett. B204 (1988) p.339.
44. W. Buchmüller and S. Cooper, in "High Energy Electron-Positron Physics", eds. A. Ali and P. Söding, World Scientific, Singapore, 1988, p. 410-487.
45. K. Königsmann, DESY 87-046 (1987).
46. J.P. Alexander, G. Bonvicini, P.S. Drell and R. Frey, Phys. Rev. D37 (1988) 56; J.P. Alexander, G. Bonvicini, P.S. Drell, R. Frey and V. Lüth, Nucl. Phys. B320 (1989) 45.
47. V.M. Aulchenko et al., Phys. Lett. 186B (1987) 432.
48. F.M. Renard, Nucl. Phys. B82 (1974) 1; N.N. Achasov, N.M. Budnev, A.A. Kozhevnikov and G.N. Shestakov, Sov. J. Nucl. Phys. 23 (1976) 320; N.N. Achasov, A.A. Kozhevnikov, M. S. Dubrovin, V.N. Ivanchenko and E. V. Pakhtusova, Int. J. Mod. Phys. A 7 (1992) 3187.
49. J. Gasser, U.-G. Meißner, Nucl. Phys. B357 (1991) 90.
50. S.R. Amendolia et al. (NA7), Nucl. Phys. B277 (1986) 168.
51. J.E. Augustin, Proc. EPS Int.Conf.on HEP, CERN, Geneva, 1979; Proc. of the 1979 Cargése Summer Institute on Quarks and Leptons, eds. M. Lévy et al., Plenum Press, New York, 1980.
52. G. D' Agostini, Preprint DESY 93-175, 1993.
53. T. Sjöstrand and M. Bengtson, Comp. Phys. Comm. 27 (1982) 243; T. Sjöstrand, Comp. Phys. Comm. 28 (1983) 229.
54. A.B. Clegg and A. Donnachie, Z. Phys. C62 (1994) 455.
55. I.B. Vasserman et al. (OLYA), Sov. J. Nucl. Phys. 30 (1979) 519.
56. I.B. Vasserman et al. (TOF), Sov. J. Nucl. Phys. 33 (1981) 709.
57. S.R. Amendolia et al. (NA7), Phys. Lett. 138B (1984) 454.
58. L.M. Barkov et al. (VEPP-2M), Preprint INP 79-117, Novosibirsk, 1979.
59. A. Quenzer et al. (DM1), Phys. Lett. 76B (1978) 512.
60. D. Bisello et al. (DM2), Phys. Lett. B220 (1989) 321.
61. G. Barbiellini et al. ($\mu\pi$), Lett. Nuovo Cim. 6 (1973) 557.
62. D. Bollini et al. (BCF), Lett. Nuovo Cim. 14 (1975) 418.
63. B. Esposito et al. (MEA), Phys. Lett. 67B (1977) 239; Lett. Nuovo Cim. 28 (1980) 337.
64. L.M. Barkov et al. (CMD), Preprint INP 89-15, Novosibirsk, 1989.
65. S.I. Dolinsky et al. (ND), Phys. Rep. C202 (1991) 99.
66. G. Cosme et al. (M2N), Phys. Lett. 63B (1976) 349; G. Parrour et al. (M2N), Phys. Lett. 63B (1976) 357.
67. G. Cosme et al. (M3N), Nucl. Phys. B152 (1979) 215; C. Paulot (M3N), Preprint LAL-79-14, Orsay, 1979.
68. B. Esposito et al. (MEA), Lett. Nuovo Cim. 28 (1980) 195.
69. A. Cordier et al. (DM1), Nucl. Phys. B172 (1980) 13.
70. A. Antonelli et al. (DM2), Z. Phys. C56 (1992) 15.
71. L.M. Kurdadze et al. (OLYA), JETP Lett. 43 (1986) 643.
72. L.M. Kurdadze et al. (OLYA), JETP Lett. 47 (1988) 512.
73. L.M. Barkov et al. (CMD), Sov. J. Nucl. Phys. 47 (1988) 248.
74. A. Cordier et al. (DM1), Phys. Lett. 109B (1982) 129.
75. D. Bisello et al. (DM2), Preprint LAL-90-71, Orsay, 1990; M. Schioppa, Thesis, Rome, 1986.
76. D. Bisello et al. (DM2), Preprint LAL-91-64, Orsay, 1991.
77. A. Cordier et al. (DM1), Phys. Lett. 106B (1981) 155.
78. A. Pais, Ann. Phys. N.Y. 9 (1960) 548.
79. C. Bacci et al. ($\gamma\gamma 2$), Phys. Lett. 86B (1979) 234.
80. D. Bisello et al. (DM1), Phys. Lett. 107B (1981) 145.
81. A. Antonelli et al. (DM2), Phys. Lett. B212 (1988) 133.
82. S.I. Dolinsky et al. (ND), Phys. Lett. B174 (1986) 453.
83. P.M. Ivanov et al. (OLYA), Phys. Lett. 107B (1981) 297.
84. P.M. Ivanov et al. (OLYA), JETP Lett. 36 (1982) 112.
85. G.V. Anikin et al. (CMD), Preprint INP 83-85, Novosibirsk, 1983; E.P. Solodov, Thesis, Novosibirsk, 1984.
86. G. Grosdidier et al. (DM1), Preprint LAL-80-35, Orsay, 1980; B. Delcourt et al. (DM1), Phys. Lett. 99B (1981) 257; F. Mane et al. (DM1), Phys. Lett. 99B (1981) 261.
87. M. Bernardini et al. (BCF), Phys. Lett. 46B (1973) 261.
88. D. Bisello et al. (DM2), Z. Phys. C39 (1988) 13.
89. A. Cordier et al. (DM1), Phys. Lett. 110B (1982) 335; F. Mane et al. (DM1), Phys. Lett. 112B (1982) 178.
90. G. Bassompierre et al., Phys. Lett. 68B (1977) 477; B. Delcourt et al. (DM1), Phys. Lett. 86B (1979) 395.
91. D. Bisello et al. (DM2), Nucl. Phys. B224 (1983) 379; Z. Phys. C48 (1990) 23.
92. A. Antonelli et al. (FENICE), Phys. Lett. B334 (1994) 431.
93. M. Ambrosio et al. ($B\bar{B}$), Phys. Lett. 91B (1980) 155.
94. B. Esposito et al. (MEA), Lett. Nuovo Cim. 19 (1977) 21; 30 (1981) 65.
95. M. Bernardini et al. (BCF), Phys. Lett. 51B (1974) 200; 53B (1974) 384.
96. P.A. Rapidis et al. (Mark I/Lead Glass Wall), Phys. Rev. Lett. 39 (1977) 526; W. Bacino et al. (Mark I/Lead Glass Wall), Phys. Rev. Lett. 40 (1978) 671.
97. J.L. Siegrist et al. (Mark I), Phys. Rev. D26 (1982) 969; J.L. Siegrist, SLAC-Report No. 225, 1979.
98. R. Brandelik et al. (DASP), Phys. Lett. 76B (1978) 361; H. Albrecht et al. (DASP), Phys. Lett. 116B (1982) 383.
99. J. Burmeister et al. (PLUTO), Phys. Lett. 66B (1977) 395; Ch. Berger et al. (PLUTO), Phys. Lett. 81B (1979) 410; L. Criegee and G. Knies (PLUTO), Phys. Rep. C83 (1982) 151.
100. B. Niczyporuk, et al. (LENA), Z. Phys. C15 (1982) 299.
101. Z. Jakubowsky et al. (Crystal Ball), Z. Phys. C40 (1988) 49; C. Edwards et al. (Crystal Ball), SLAC-PUB-5160, 1990.
102. A.E. Blinov et al. (MD-1), Z. Phys. C49 (1991) 239; A.E. Blinov et al. (MD-1), Preprint BudkerINP 93-54, Novosibirsk, 1993.
103. H. J. Behrend et al. (CELLO), Phys. Lett. B183 (1987) 400.
104. W. Bartel et al. (JADE), Phys. Lett. 129B (1983) 145; 160B (1985) 337; B. Naroska et al. (JADE), Phys. Rep. C148 (1987) 67.
105. B. Adeva et al. (MARK J), Phys. Rev. Lett. 50 (1983) 799, 2051; Phys. Rep. C109 (1984) 131; Phys. Rev. D34 (1986) 681.
106. R. Brandelik et al. (TASSO), Phys. Lett. 113B (1982) 499; M. Althoff et al. (TASSO), Phys. Lett. 138B (1984) 441 .
107. P. Bock et al. (DHHM), Z. Phys. C6 (1980) 125.
108. R. Giles et al. (CLEO), Phys. Rev. D29 (1984) 1285; D. Besson et al. (CLEO), Phys. Rev. Lett. 54 (1985) 381.
109. E. Rice et al. (CUSB), Phys. Rev. Lett. 48 (1982) 906.
110. D. Bender et al. (HRS), Phys. Rev. D31 (1985) 1.
111. E. Fernandez et al. (MAC), Phys. Rev. D31 (1985) 1537.
112. Numerical Data and Functional Relationships in Science and Technology: Group. 1: Nuclear and Particle Physics. Vol. 14: Electron - Positron Interactions, by H. Schopper, (ed.), D.R.O. Morrison, V.V. Ezhela, Yu.G. Stroganov, O.P. Yushchenko, V. Flaminio, (ed.) , M.R. Whalley, (ed.), Springer, Berlin, 1992 (Landolt-Boernstein. New Series, 1.14).
113. T.H. Chang, K.J.F. Gaemers and W.L.V. van Neerven, Nucl. Phys. B202 (1982) 407.
114. N.A. Papadopulos, J.A. Peñarrocha, F.Scheck and K. Schilcher, Phys. Lett. 140B (1984) 213; Nucl. Phys. B258 (1985) 1.
115. V.A. Novikov, L.B. Okun and M.I. Vysotskii, Phys. Lett. B324 (1994) 89.
116. B.V. Geshkenbein and V.L. Morgunov, Phys. Lett. B340 (1994) 185; Preprint ITEP-70-94, 1994.
117. E. Pallante, Phys. Lett. B341 (1994) 221.
118. F. Jegerlehner and J. Fleischer, Phys. Lett. 151B (1985) 65; Acta Phys. Polonica B17 (1986) 709.

119. B.I. Khazin, Talk given at 27th International Conference on High Energy Physics (ICHEP), Glasgow, Scotland, 20-27 July 1994.
120. Paolo Franzini, The Muon Gyromagnetic Ratio and R_H at DAΦNE, in the "Second DAΦNE Physics Handbook", ed. L. Maiani, L. Pancheri and N. Paver, to appear, 1995.

This article was processed by the author using the LaTeX style file *cljour2* from Springer-Verlag.